NASA Technical Memorandum 85706

DEC 1983
RECEIVED
NASA STI FACILITY
ACCESS DEPT.

VERTICAL DROP TEST OF A TRANSPORT FUSELAGE CENTER SECTION INCLUDING THE WHEEL WELLS

M. SUSAN WILLIAMS
ROBERT J. HAYDUK

OCTOBER 1983

(NASA-TM-85706) VERTICAL DROP TEST OF A TRANSPORT FUSELAGE CENTER SECTION INCLUDING THE WHEEL WELLS (NASA) 59 p HC A04/MF A01 N84-12531
CSCL 20K Unclas
G3/39 42555

National Aeronautics and
Space Administration

Langley Research Center
Hampton, Virginia 23665

VERTICAL DROP TEST OF A TRANSPORT FUSELAGE CENTER SECTION INCLUDING THE WHEEL WELLS

M. Susan Williams
Robert J. Hayduk

Langley Research Center

Summary

A 13-foot long Boeing 707 fuselage section was drop-tested at the NASA Langley Research Center to measure structural, seat and occupant response to vertical crash loads. Occupant response was simulated with anthropomorphic dummies. The specimen had nominally zero pitch, roll, and yaw at impact with a sink speed of 20 ft/sec. Results from this drop test and other drop tests of different transport sections will be used to prepare for a full-scale crash test of a B-720 in July, 1984.

Post-test inspection showed no apparent damage to the stiff fuselage structure during the test, however, seat frame bending failures and seat pan attachment failures occurred to the onboard seats. Preliminary data traces indicated maximum normal accelerations of 70 g at the fuselage bottom, 70 to 95 g at the cabin floor, and 44 g at the dummy pelves.

INTRODUCTION

As part of the NASA LaRC Transport Crash Test program, reference 1, various fuselage sections from Boeing 707 transport aircraft were acquired for dynamic drop testing. The structural response data from these tests will be used to corroborate the DYCAST computer program, reference 2, being developed for crash analysis of aircraft structures. Another purpose of these tests is to determine structural, seat, and occupant response to vertical crash loads in preparation for a full-scale crash test of a remotely piloted B-720 to be conducted at NASA Dryden Flight Research Facility in July, 1984 as part of a joint NASA/FAA program.

This report presents photographs and preliminary data traces from the second Transport Section Drop Test conducted June 8, 1983. This 13-foot long, 14.2-foot high section located at the rear of the wing and including the wheel wells, keel beam, and part of the rear wing spar (see Fig. 1) was drop-tested at 20 ft/sec using the Vertical Test Apparatus at NASA Langley Research Center. The first section, located just forward of the wing, was tested under identical conditions on April 26, 1983 (Ref. 3). Results from these tests will provide an indication of vertical loads and accelerations to be expected in the full-scale crash test of the B-720.

TEST SPECIMEN

The fuselage section is shown suspended in the Vertical Test Apparatus at the Impact Dynamics Research Facility in figure 2. The 13-foot long section was cut from a Boeing 707 10-in forward of Body Station (BS) 820 to 10-in aft of BS 960 (Fig. 1) (Ref. 4). After removing nonstructural items, such as interior paneling, insulation, storage bins, ducting, etc., the bare section weighed 5400 lbs. The section weighed 7964 lbs when loaded with seats, anthropomorphic dummies, and instrumentation.

Figure 3 is a floor layout of seats, instrumentation junction box, a simulated power distribution pallet (for weight simulation) and a battery for camera power. Seats were located on the test section approximately as they are to be located on the full-scale airplane test. All seats were standard triple transport seats. They were surplus seats that were purchased with the transport sections and were used to apply the proper load factor to the floor. Eight 50th percentile, 165 lb, Part 572 anthropomorphic dummies (Ref. 5) were distributed among the four triple seats (designated as seats B, C, D, and E in Fig. 3) as follows:

Seat	Anthropomorphic Dummy Location
B	Center, Inboard
C	Center, Outboard
D	Center
E	Inboard, Center, Outboard

All dummies had normal (aligned with the spine), longitudinal (fore-and-aft perpendicular to the spine), and transverse (left and right perpendicular to the spine) accelerometers in their pelves. In addition, a normal accelerometer was in the head of each dummy. A 95th percentile dummy (195 lb) sat in the inboard location of seat D but was not instrumented with accelerometers. Each of the remaining three occupant locations were loaded with approximately 130 lb of weight (see Fig. 4). This weight represents 80 percent of the total weight of a 50th percentile occupant assuming the legs (20 percent of the total weight) do not load the seat pan. Table I gives the weight and coordinates of all articles onboard the test section. The origin (0,0,0) was chosen to be along the centerline of the fuselage (X), 10-in forward of BS 820 (front edge of section) (Y), and on top of the floor (Z). Positive axes directions were forward (X), to the right (Y), and down (Z). Figure 5 gives the seat leg locations in inches relative to the front edge of the test section floor.

TEST APPARATUS AND METHODS

The NASA Vertical Test Apparatus (VTA) (Fig. 1) was used to drop-test the transport section and to provide a stable guide mechanism for the vertical impact test. The VTA was designed for the following conditions:

1. Maximum impact velocity - 50 ft/sec

2. Maximum specimen dimensions - 12 ft diameter, 26 ft long, 10,000 lb weight

Test conditions for the transport section test fell below these limits.

The VTA is located at the northwest leg of the gantry structure at the Impact Dynamics Research Facility (Ref. 6). The gantry provides support through lateral ties to the VTA. The VTA (70 ft high) consists of a 7 1/2 ton hoist platform on two support columns. Each column has rails to guide the vertical motion of a lift frame to which a specimen can be attached for drop testing. A power quick release hook is used to lift the support frame and specimen to the desired drop height. The specimen impacts a steel reinforced concrete pad at the bottom of the VTA while the support frame is decelerated by impacting shock absorbers.

For the transport section test, the section was connected to the support frame by a series of cables with turnbuckles to adjust cable length and control the impact attitude. The impact attitude for the test was 0 degree pitch, 0 degree yaw, and 0 degree roll. The section was raised 6 ft 2.5 in above the impact surface to obtain a vertical impact velocity of 20 ft/sec. The section contacted the concrete prior to the support frame impacting the shock absorbers.

INSTRUMENTATION AND DATA REDUCTION

DC accelerometers were used in the dummies and on the aircraft structure to obtain continuous recordings during the dynamic drop test. The accelerometers were mounted on aluminum blocks, which were then mounted to the structure (Fig. 6). Seat E (see Fig. 3) was mounted on four load cells to measure normal and longitudinal reaction forces at the seat leg attachment points. Figures 7a and 7b show the location of the accelerometers on the aircraft structure and the positive axes directions. All data were transmitted to a tape recorder through an umbilical cable that was hard-wired to the data aquisition system.

The analog signals were filtered during recording at 600 Hz and subsequently digitized at 4000 samples per second. The digitized accelerometer data were passed through the following digital filters:

Dummy Head	180 Hz
Dummy Pelvis	180 Hz
Aircraft Structure	60 Hz
Load Cells	60 Hz

Motion pictures were taken at 400 pictures per second during the experiment. The cameras were located onboard the test section and on the ground. Still photographs were taken before and after the test.

GENERAL RESULTS

Figures 8a and 8b show post-test damage to the transport section. The frontal view of the section in figure 8a shows that no apparent damage occurred to the fuselage during the test. This is an extremely stiff structure, which did not deform during the impact test; consequently, high loads were transmitted from the lower fuselage into the floor, upper fuselage, seats, and anthropomorphic dummies. Bending failures developed along the lateral support tube of the seat frame of seats B, C, and D (see Fig. 8b). The tube failed where the inboard and outboard seat locations are cantilevered over the seat legs. The failures occurred only at the seat locations that were loaded with ballast to simulate the weight of an anthropomorphic dummy. Obviously, the weights distributed the load over the seat frame differently than the anthropomorphic dummy. In the seat locations with dummies, failures occurred where the rubberized seat pans attached to the seat frame. High acceleration levels transmitted through the structure caused the onboard lights to fail (lighting for onboard cameras) and one camera to disconnect from its mount during impact.

Acceleration time histories for the structure and anthropomorphic dummies are given in figures 9a through 9s and 10a through 10p, respectively. The locations of the structural acceleromters are identified by word descriptions and by numbers, which are shown in figures 7a and 7b. The locations of the accelerometers in the dummies are also identified by word descriptions and by numbers referring to figure 3. Figures 11a through 11d show normal and longitudinal reaction forces measured at the seat attachment points for seat E. The letters N, L, and T on the data traces indicate normal, longitudinal, and transverse directions respectively. For the structural accelerometers and load cells, N, L, and T correspond to the Z, X, and Y axes of the transport section. However, for the anthropomorphic dummies, N, L, and T are relative to the dummy axis system as described in the Test Specimen section. These data traces are presented in an unrefined form in order to make them available quickly.

The maximum normal acceleration of the major pulse measured on the keel beam and wheel well walls and ceiling was approximately 71 g (60 Hz filter) for a time duration of 0.019 sec. Since no crushing of the lower fuselage occurred during impact, accelerations at the floor beams were of the same magnitude or higher than those measured at the lower fuselage. Maximum normal accelerations measured at the floor beam / inboard seat rail location were about 70 g (60 Hz filter) for 0.022 sec while those measured at the floor beam / frame location were higher, averaging 95 g (60 Hz filter) for 0.017 sec. The maximum normal pelvis acceleration for the dummies was approximately 44 g (filtered at 180 Hz) for 0.049 sec.

The maximum normal acceleration level measured at the roof was similar in magnitude to that at the floor beam / frame location. However, the roof normal accelerometers at BS 860 and 920 (Figures 9a and 9b) show an oscillatory rather than pulse response, as exhibited on the floor and undercarriage. Nearly 93 g (60 Hz filter) for 0.024 sec was measured during the first half wave at BS 860. The oscillatory response at the roof is in the 24 to 27 cycle per second range.

Figures 11a through 11d show forces measured by load cells at the seat attachment points of seat E. Compressive forces at the front legs ranged from 3200 to 4200 lbs in the normal direction. Since the front legs are mainly vertical, little force was applied in the longitudinal direction for a vertical impact. In contrast, the rear legs are angled and normal forces in the legs ranged from 2140 to 2860 lbs (compression) and longitudinal forces ranged from 960 to 1320 lbs.

CONCLUDING REMARKS

A Boeing 707 fuselage section was drop tested at the Impact Dynamics Research Facility, NASA Langley Research Center, to study structural, seat, and occupant response to vertical crash loads in preparation for a full-scale crash test of a B-720 in July, 1984. The section, located at the rear of the wing and including the wheel wells, keel beam, and part of the rear wing spar, was tested at 20 ft/sec vertical impact velocity without roll, pitch, or yaw.

From post-test inspection of the fuselage section and preliminary data traces the following were concluded:

1. No damage occurred to the fuselage or floor during the impact. High loads were transmitted from the lower fuselage to the floor, seats, anthropomorphic dummies, and upper fuselage.

2. Bending failures developed in several seats along the lateral support tubes of the seat frame where the seat is cantilevered over the legs. The failures occurred only at the seat locations where ballast was used in the seat to simulate the weight of an anthropomorphic dummy.

3. At other seat locations where anthropomorphic dummies were loading the seat, failures occurred where the rubberized seat pans attach to the seat frame.

4. A maximum normal acceleration of 71 g (60 Hz filter) was measured on the fuselage bottom.

5. Maximum normal acceleration at the floor beam / inboard seat rail was 70 g (60 Hz filter) while at the floor beam / frame it was 95 g (60 Hz filter).

6. Maximum normal pelvic acceleration measured in the

anthropomorphic dummies was 44 g (180 Hz filter).

This is a quick release of technical information before complete refinement and evaluation. Consequently, the above conclusions are preliminary and subject to reconsideration.

REFERENCES

1. Thomson, Robert G., and Caiafa, Caesar: Designing for Aircraft Structural Crashworthiness. J. of Aircraft, Vol. 19, Number 10, Oct. 1982, Page 868.

2. Hayduk, R.J.; Winter, R.; Pifko, A.B.; and Fasanella, E.L.: Application of the Non-linear Finite Element Computer Program 'DYCAST' to Aircraft Crash Analysis. Structural Crashworthiness, Edited by N. Jones and T. Wierzbicki, Butterworth & Co. Ltd., 1983, pp. 283 - 307.

3. Williams, M. Susan; and Hayduk, Robert J.: Vertical Drop Test of a Transport Fuselage Section Located Forward of the Wing. NASA TM 85679, August 1983.

4. Boeing 707-720 Reference Guide D6-40942, March 1980, Boeing Commercial Airplane Company.

5. U. S. Code of Federal Regulations, Title 49, Chapter 5, Part 572: Anthropomorphic Test Dummy. Government Printing Office, Washington, D.C., (Rev.) 1978.

6. Vaughan, Victor L.; and Alfaro-Bou, Emilio: Impact Dynamics Research Facility for Full-Scale Aircraft Crash Testing. NASA TN D-8179, 1976.

TABLE I.- TRANSPORT SECTION TEST WEIGHT DISTRIBUTION

Item	Weight(lbs.)	Approximate C. G. Coordinates X(in)	Y(in)	Z(in)
Empty weight	5400	-64	0	0
Seat B: inboard	187	-35	-19	-24
center	188	-35	-38	-24
outboard	147	-35	-57	-24
Seat C: inboard	147	-35	19	-24
center	188	-35	38	-24
outboard	187	-35	57	-24
Seat D: inboard	217	-106	-19	-24
center	188	-106	-38	-24
outboard	147	-106	-57	-24
Seat E: inboard	187	-106	19	-27
center	188	-106	38	-27
outboard	187	-106	57	-27
Junction box	60	-135	36	-4
Pallet	135	-135	-36	-5
Left front camera & mount	30	-21	-41	-68
Left front light & mount	6	-23	-30	-82
Right front camera & mount	30	-21	41	-69
Right front light & mount	6	-25	30	-85
Left rear camera & mount	30	-98	-41	-68
Left rear light & mount	6	-99	-30	-82
Right rear camera & mount	30	-62	41	-68
Right rear light & mount	6	-58	30	-82
Camera on floor & mount	20	-18	19	-3
Battery	18	-155	56	-3
Camera timing panel	4	-140	70	-24
Wood foot rest for dummies in Seat E	25	-88	39	-2

ORIGINAL PAGE IS
OF POOR QUALITY

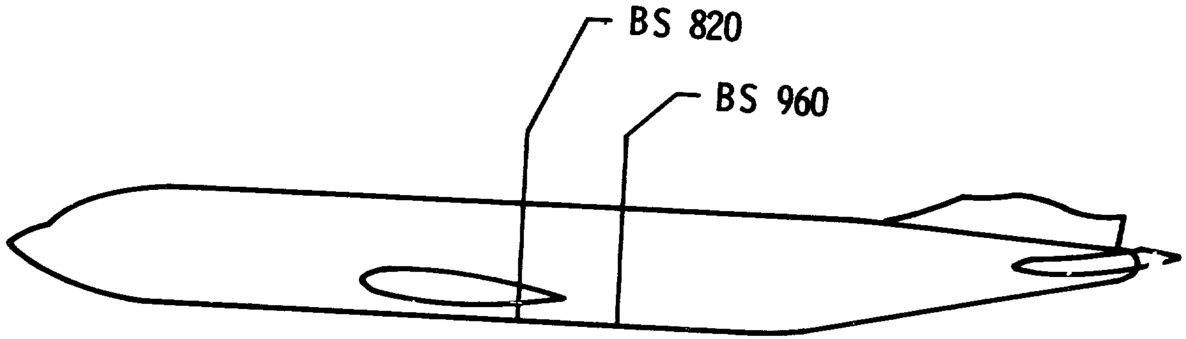

Figure 1.- B-720 fuselage showing location of test section.

ORIGINAL PAGE IS
OF POOR QUALITY

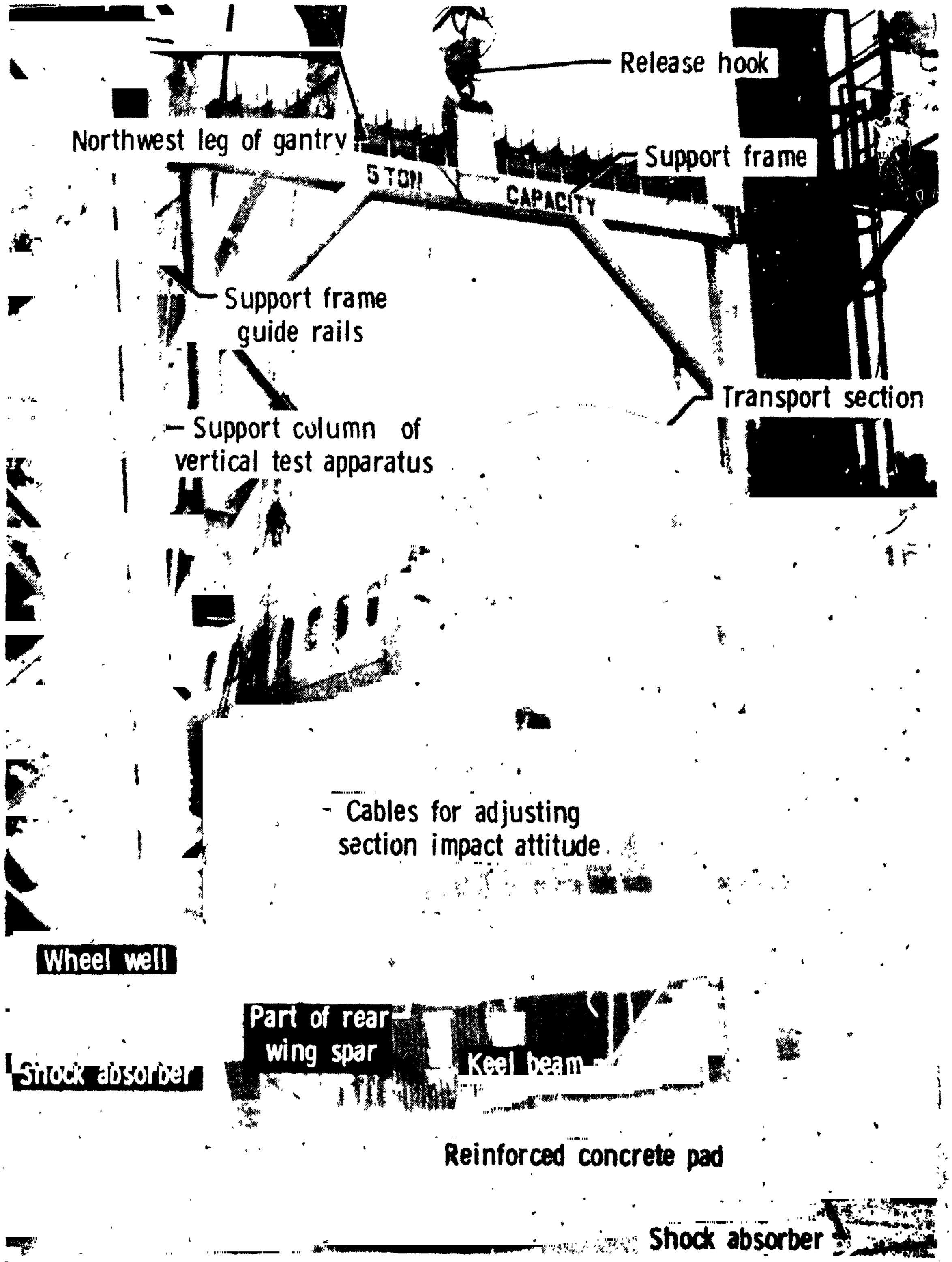

Figure 2.- Transport section suspended in Vertical Test Apparatus.

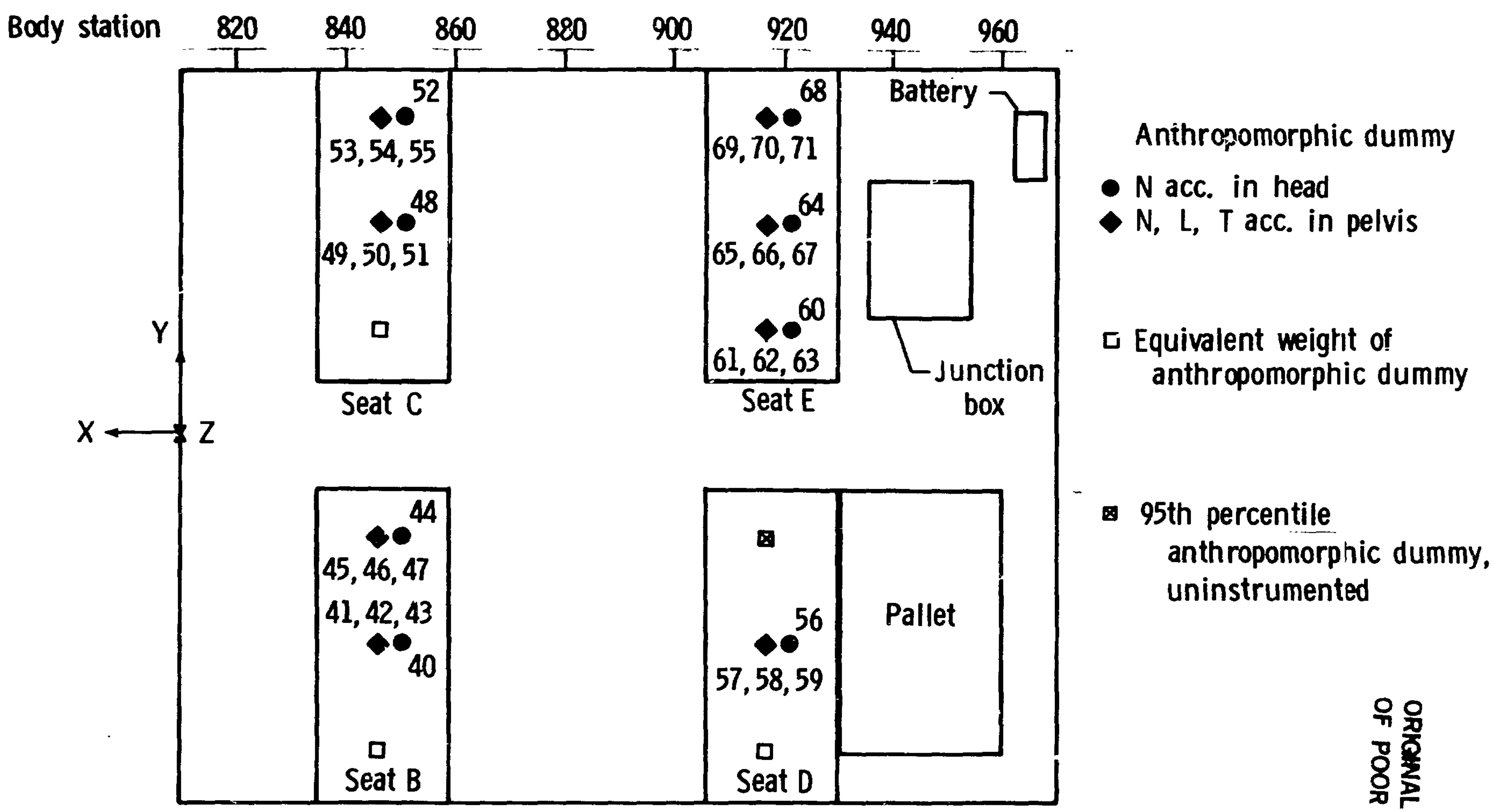

Figure 3.- Transport section test seat arrangement and accelerometer channel number identification for dummies.

ORIGINAL PAGE IS OF POOR QUALITY

ORIGINAL PAGE IS
OF POOR QUALITY

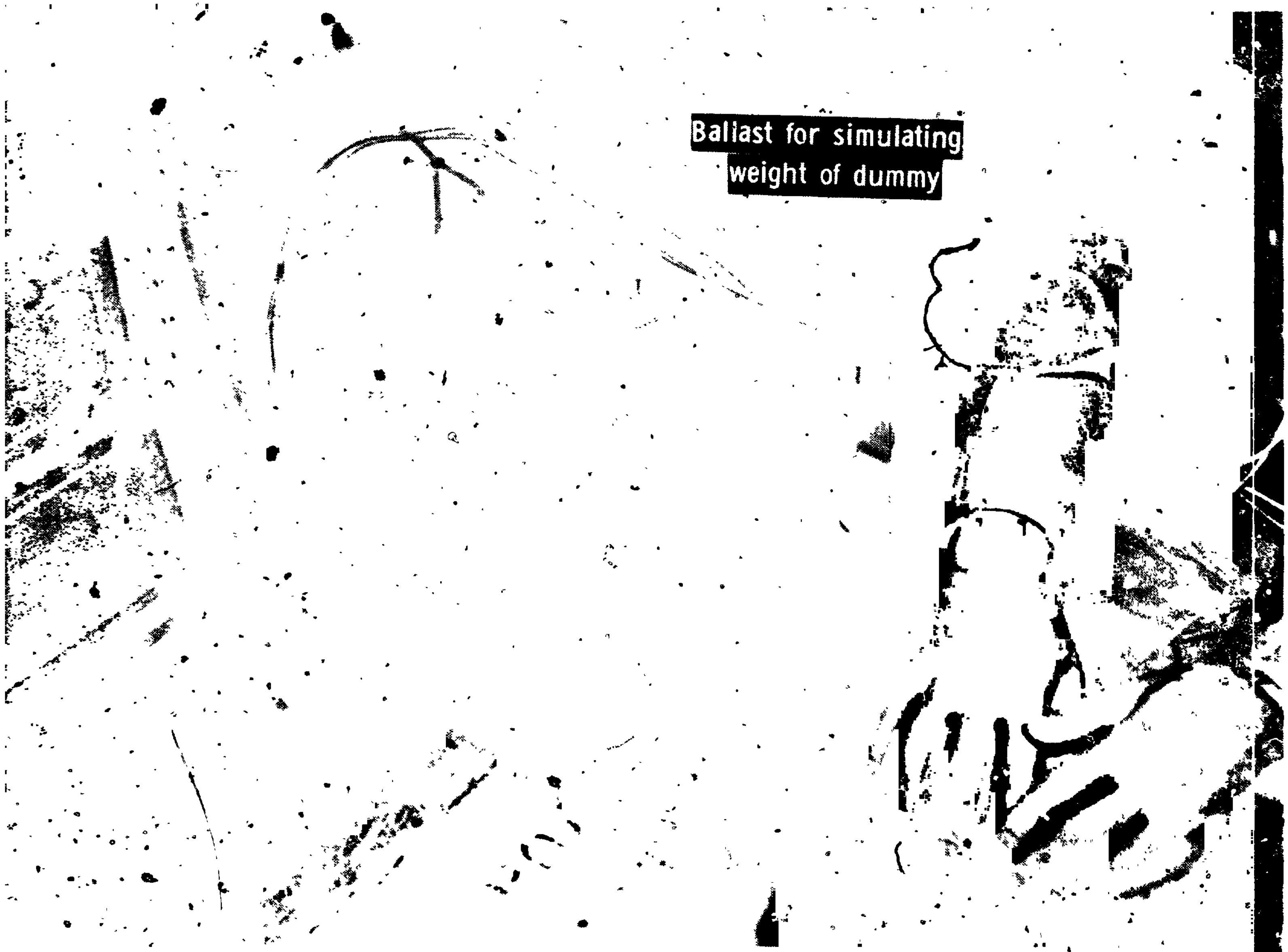

Figure 4.- Ballast used to load seats not occupied by dummies.

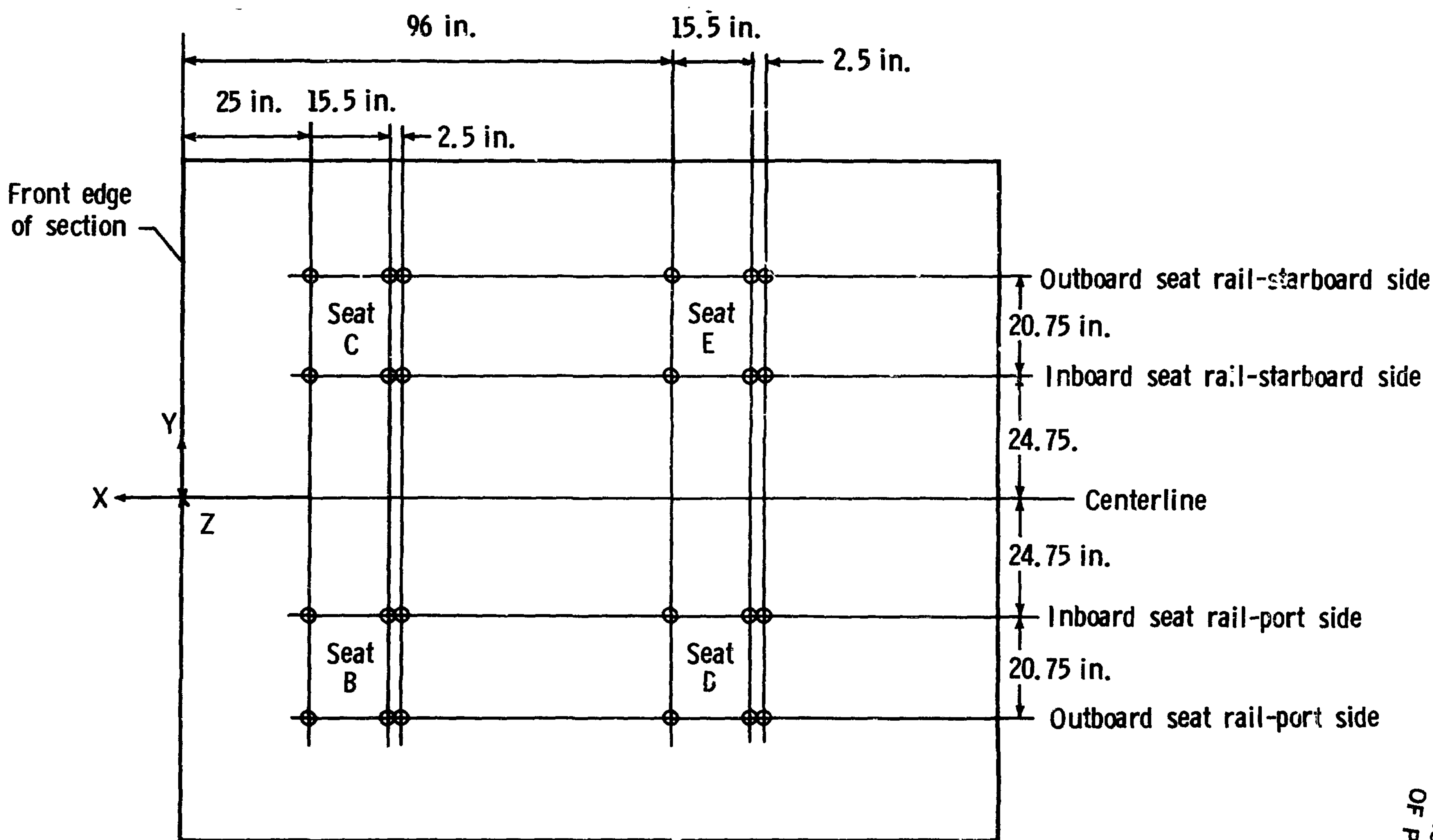

Figure 5.- Seat leg locations relative to front edge of section.

ORIGINAL PAGE IS
OF POOR QUALITY

ORIGINAL PAGE IS
OF POOR QUALITY

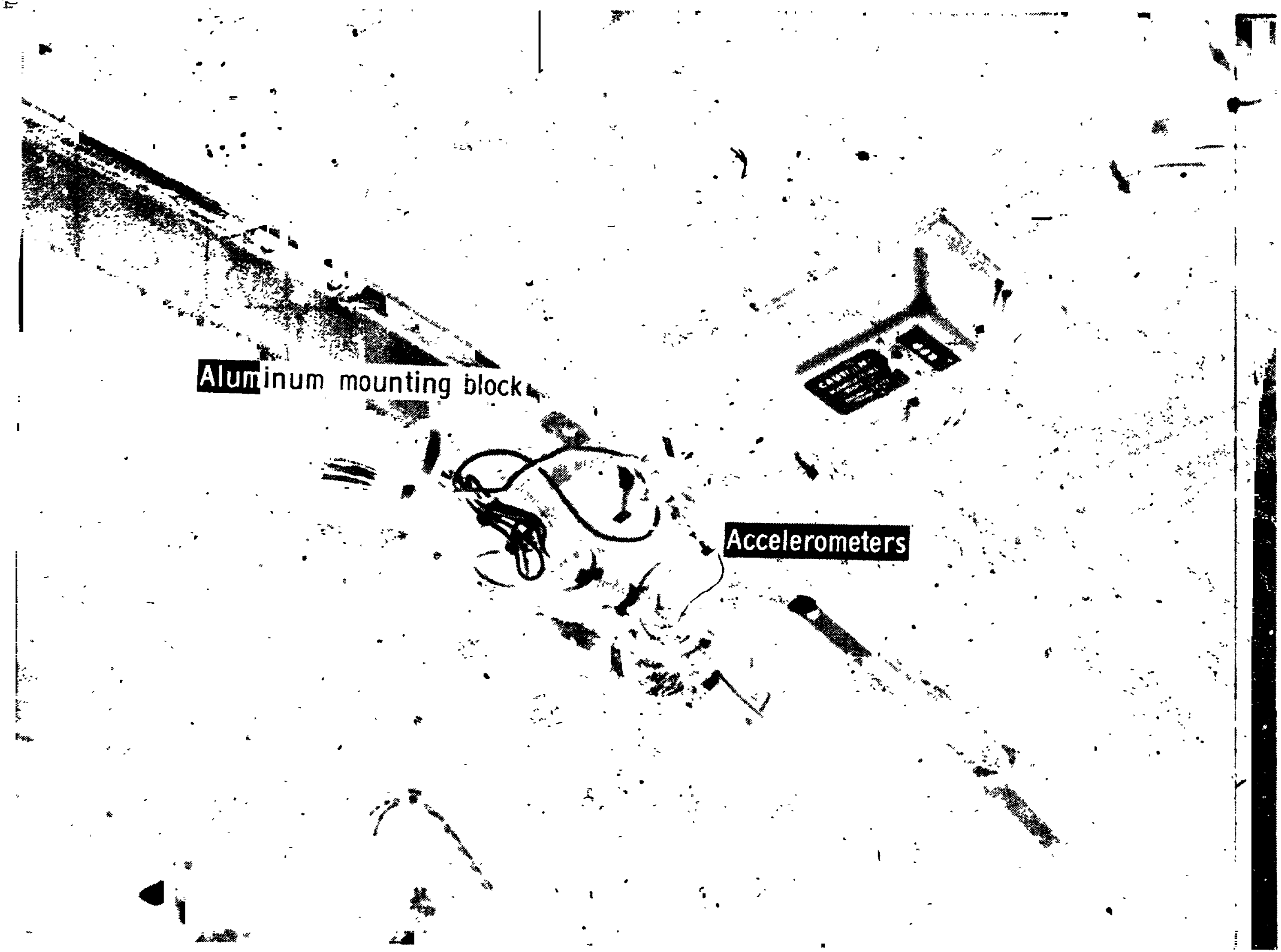

Figure 6.- Method of mounting accelerometers.

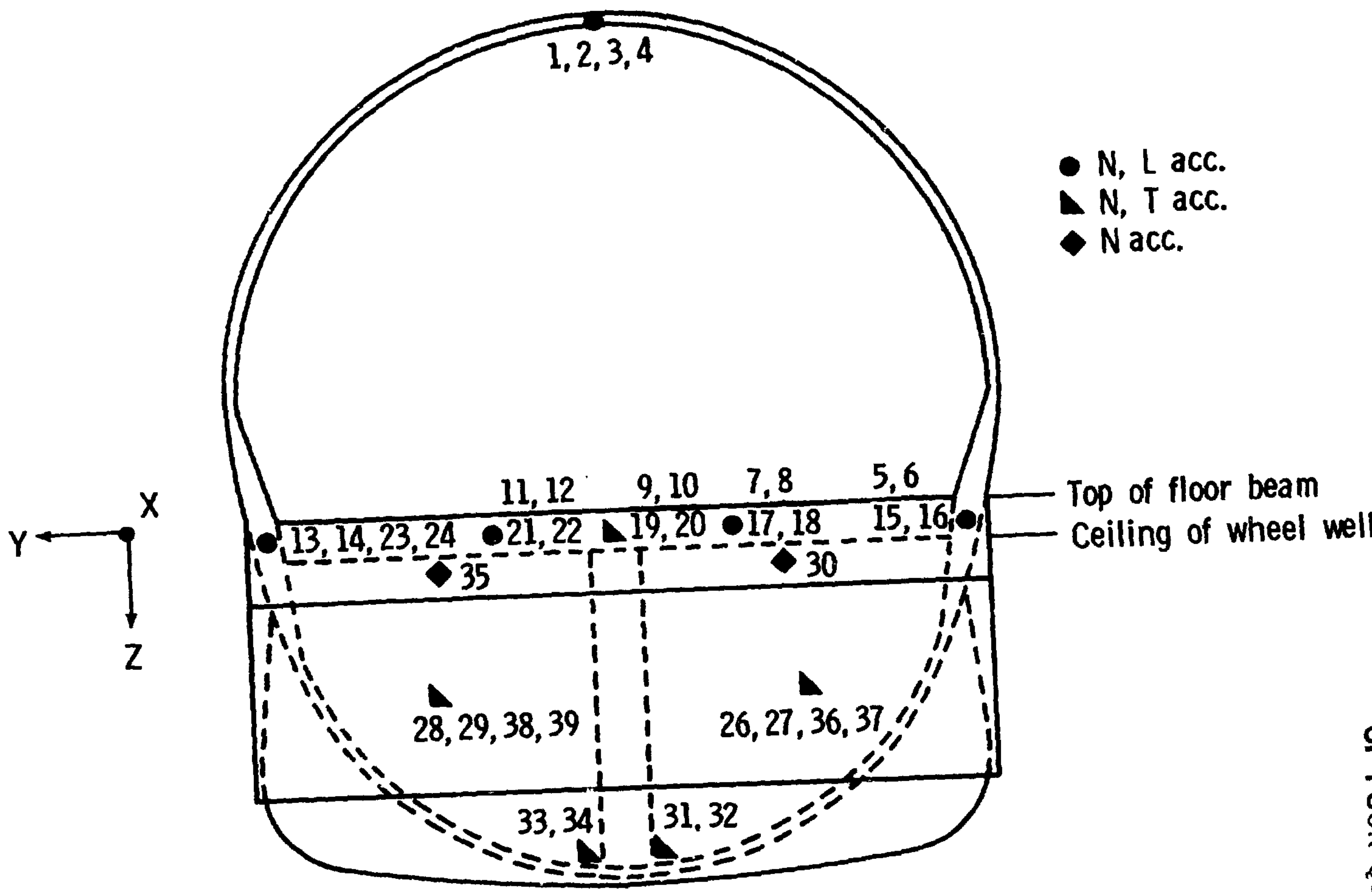

ORIGINAL PAGE IS
OF POOR QUALITY

(a) End view.

Figure 7.- Instrumentation locations for transport section test.

ORIGINAL PAGE IS
OF POOR QUALITY

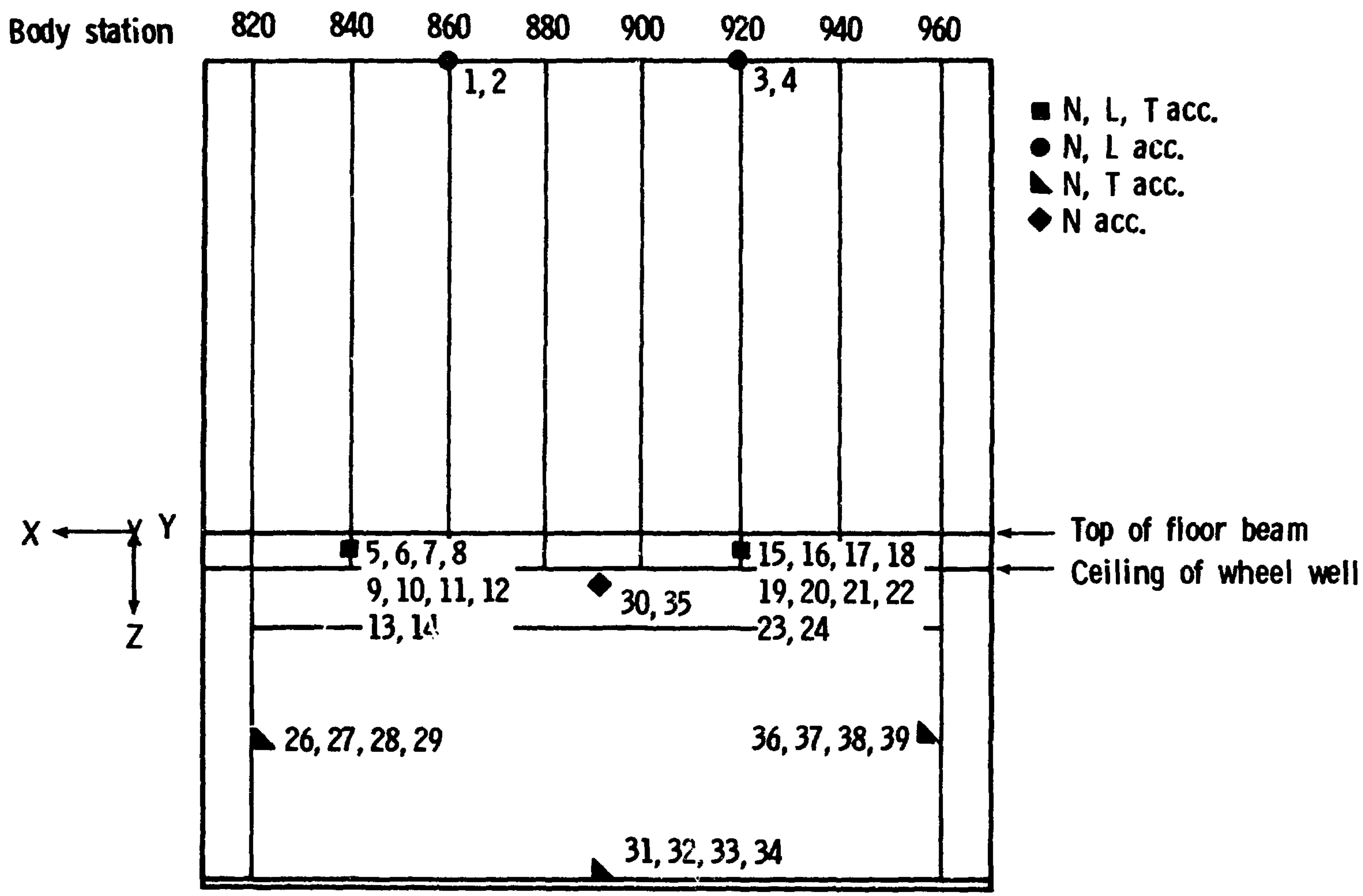

(b) Side view.

Figure 7.- Concluded.

ORIGINAL PAGE IS
OF POOR QUALITY

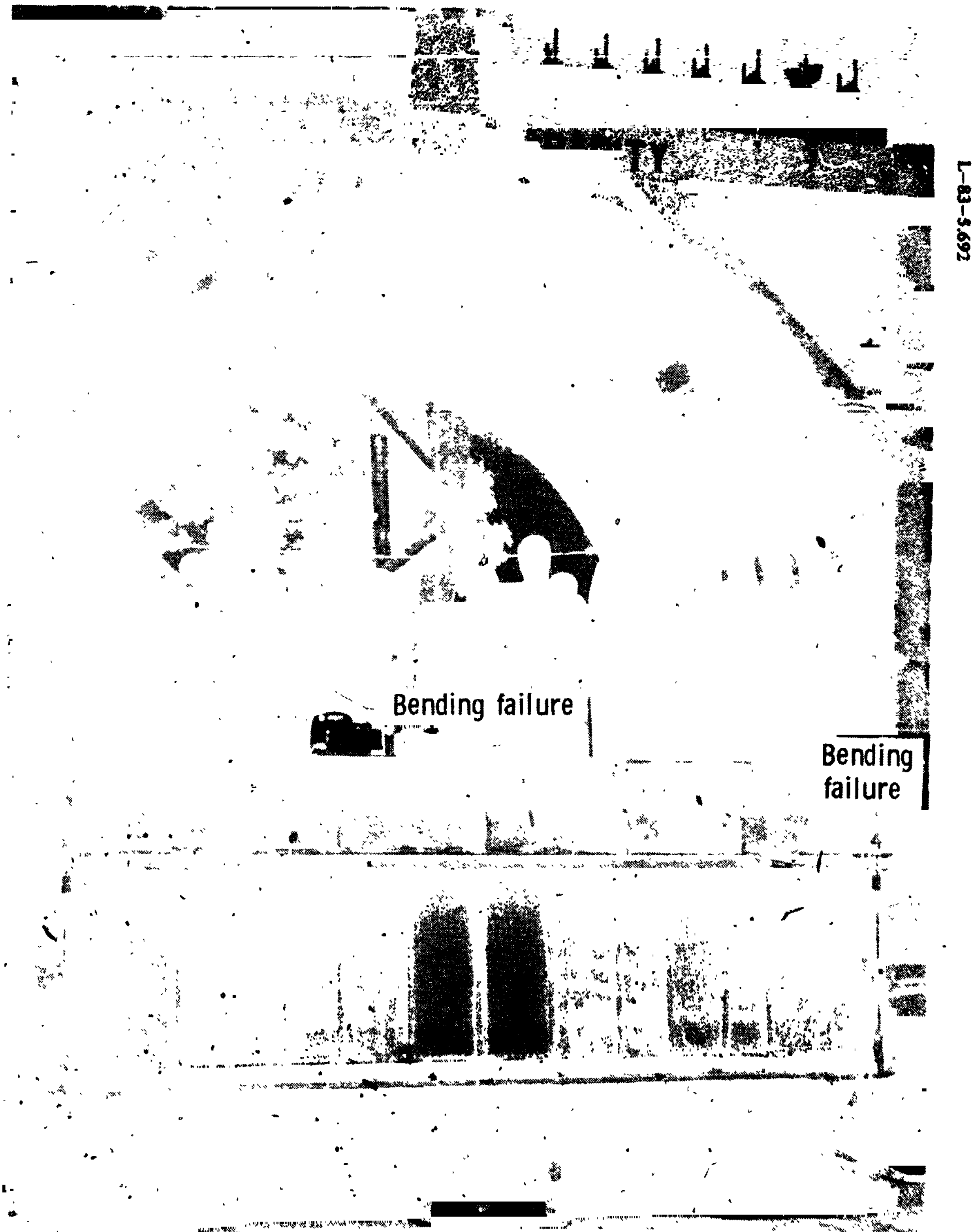

(a) Frontal view of section post-test.

Figure 8.- Post-test photographs of transport section test.

ORIGINAL PAGE IS
OF POOR QUALITY

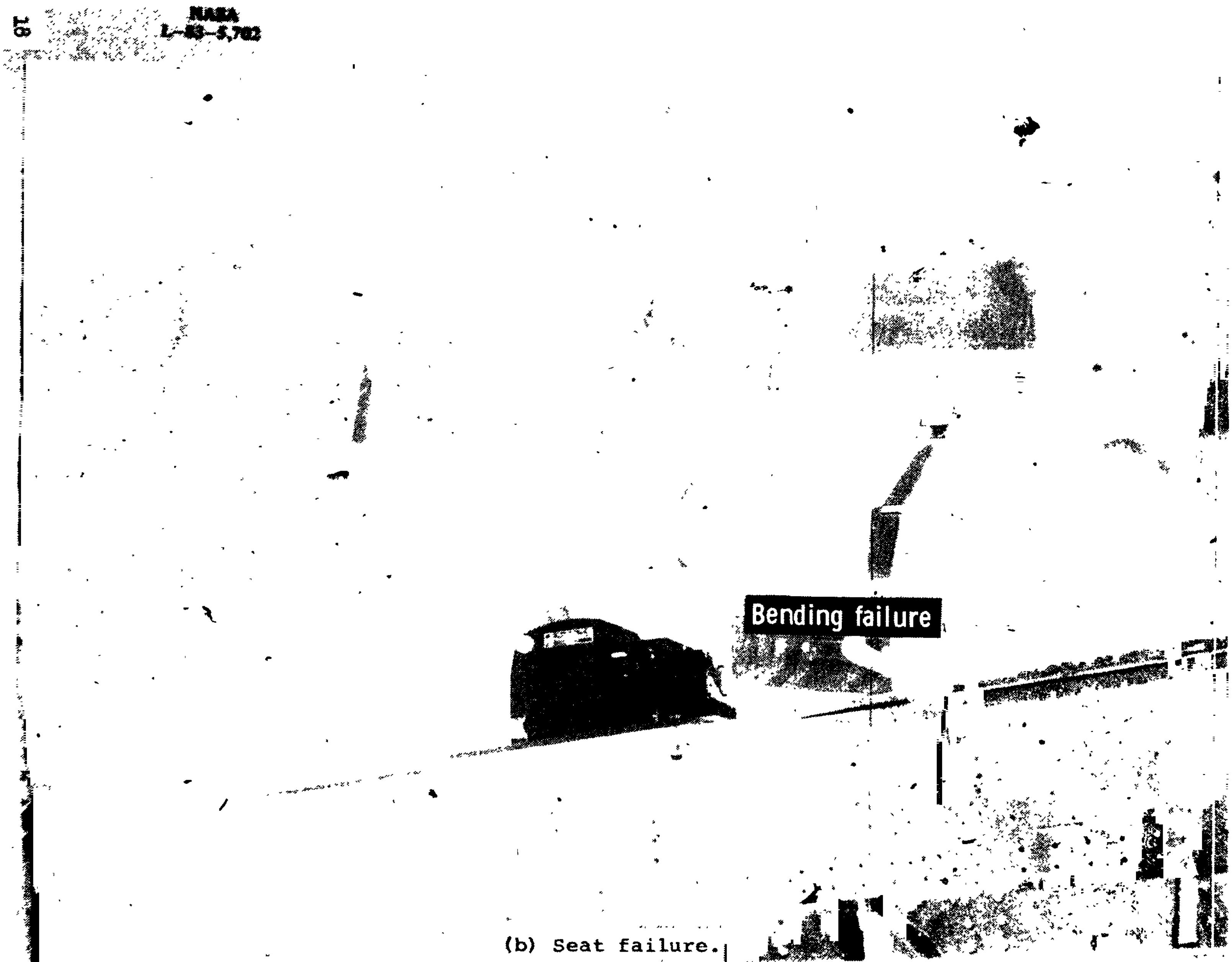

(b) Seat failure.

Figure 8.- Concluded.

ORIGINAL PAGE IS
OF POOR QUALITY

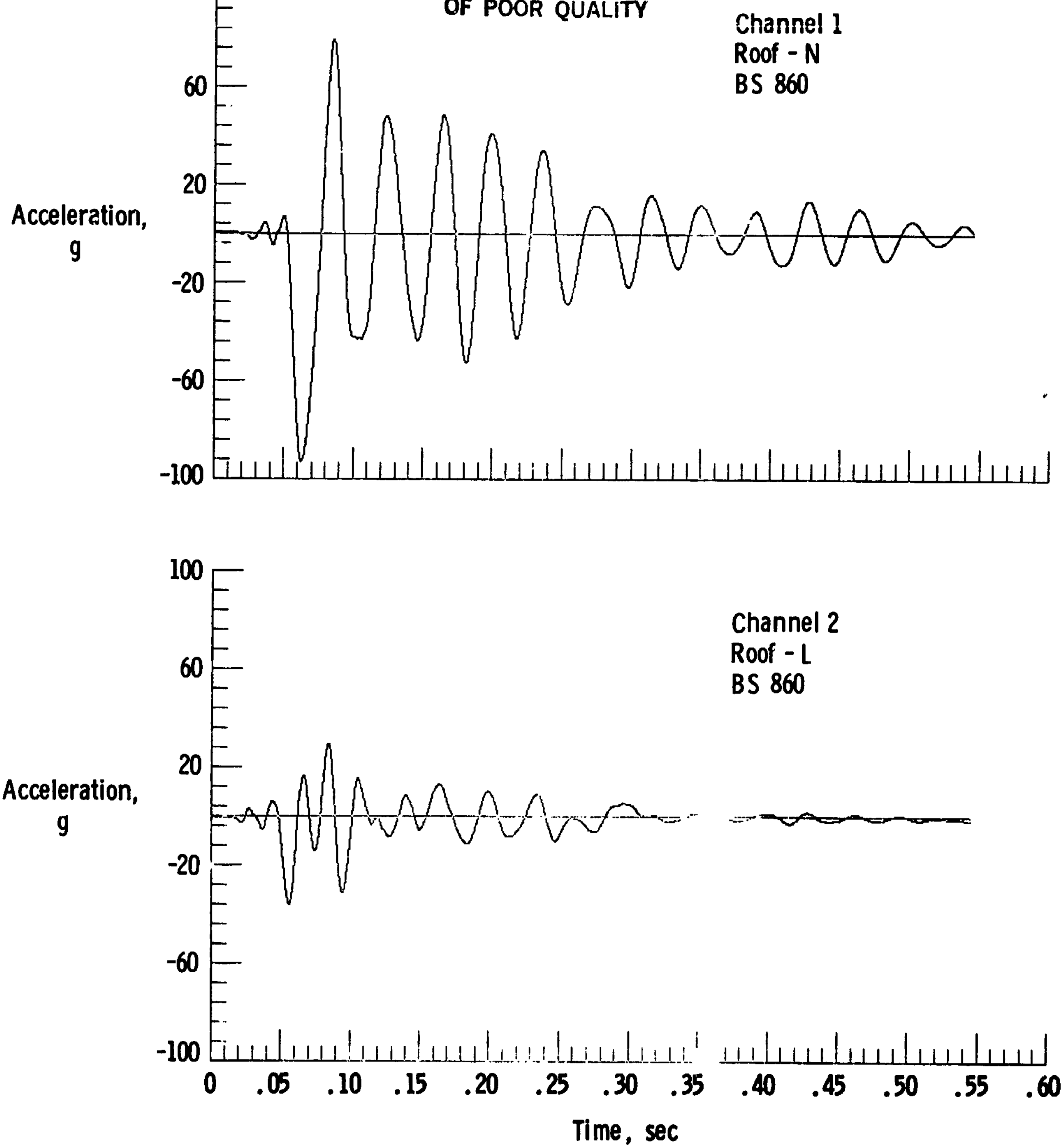

(a) Structural acceleration time histories.

Figure 9.- Acceleration time histories measured on the aircraft structure.

ORIGINAL PAGE IS
OF POOR QUALITY

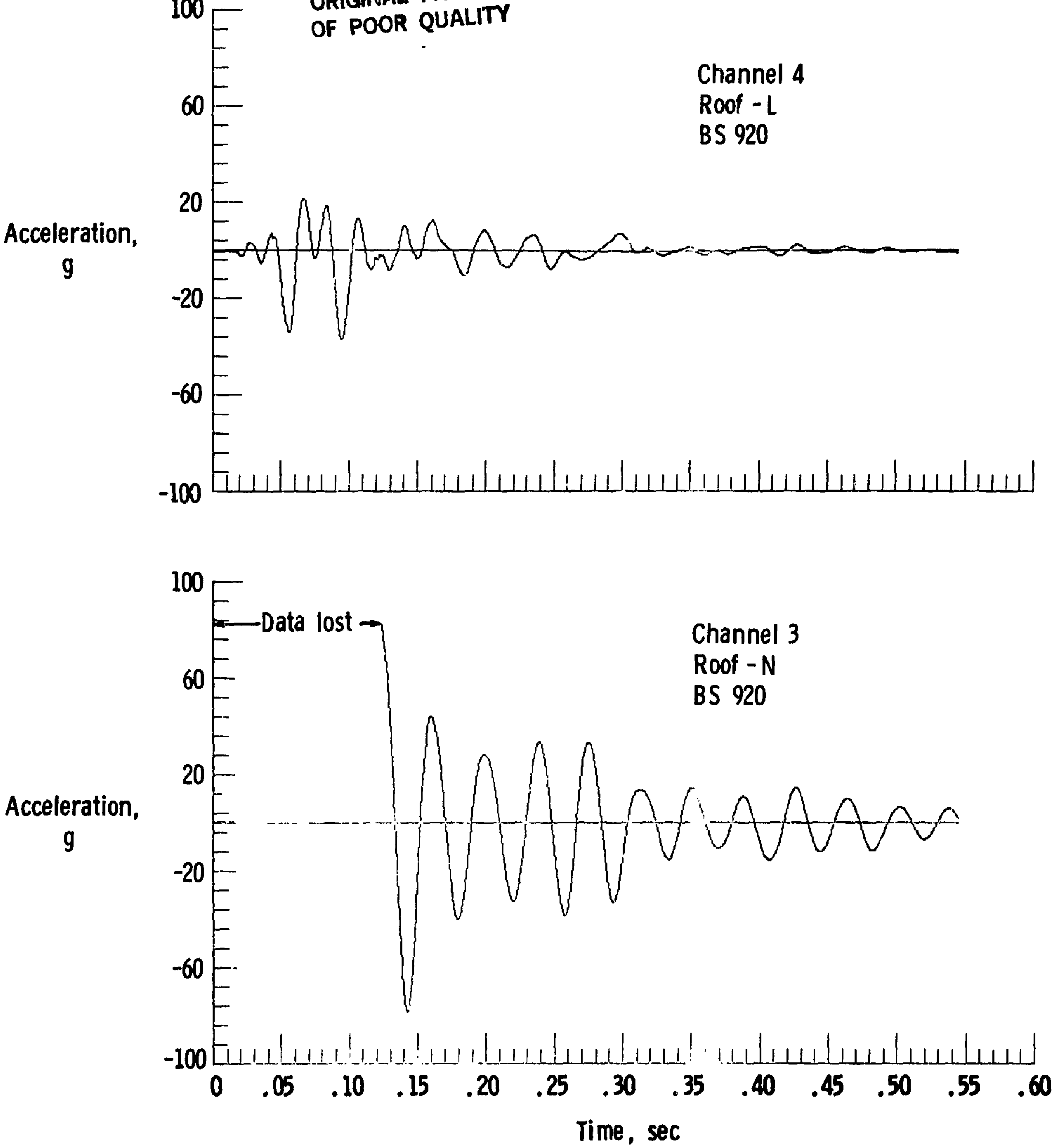

Figure 9.- Continued.

(b) Structural acceleration time histories.

ORIGINAL PAGE IS
OF POOR QUALITY

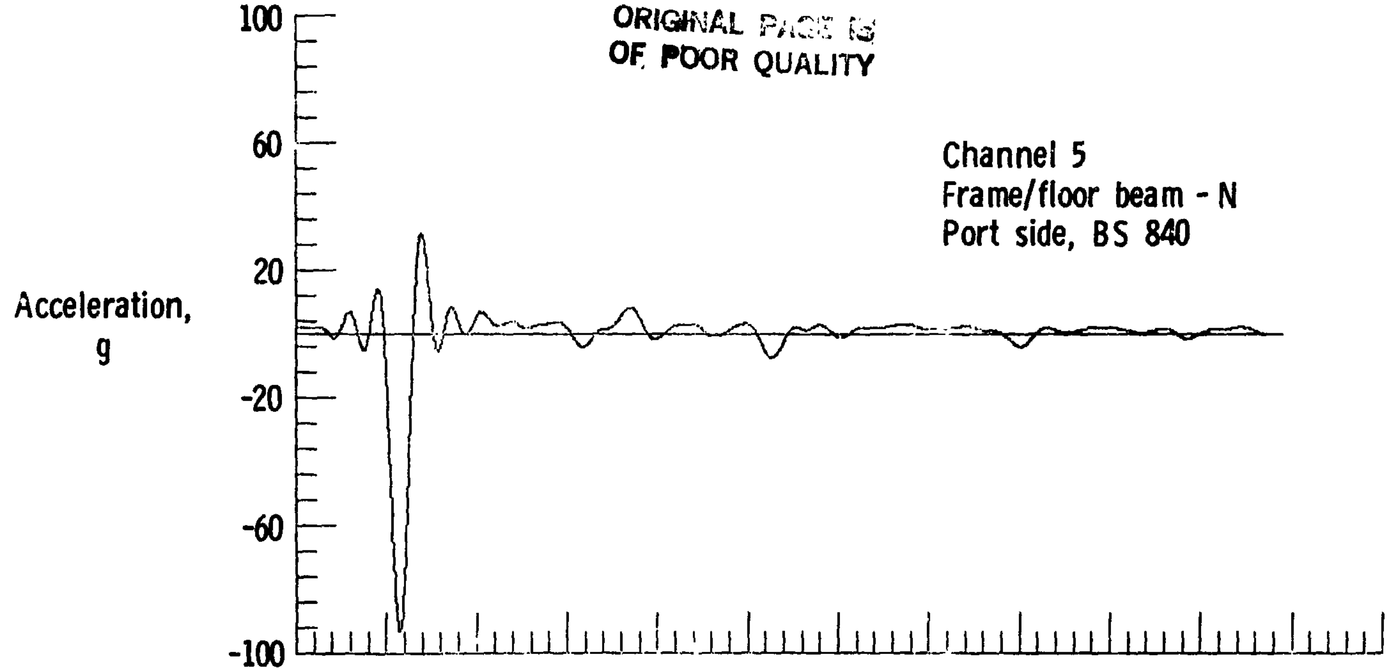

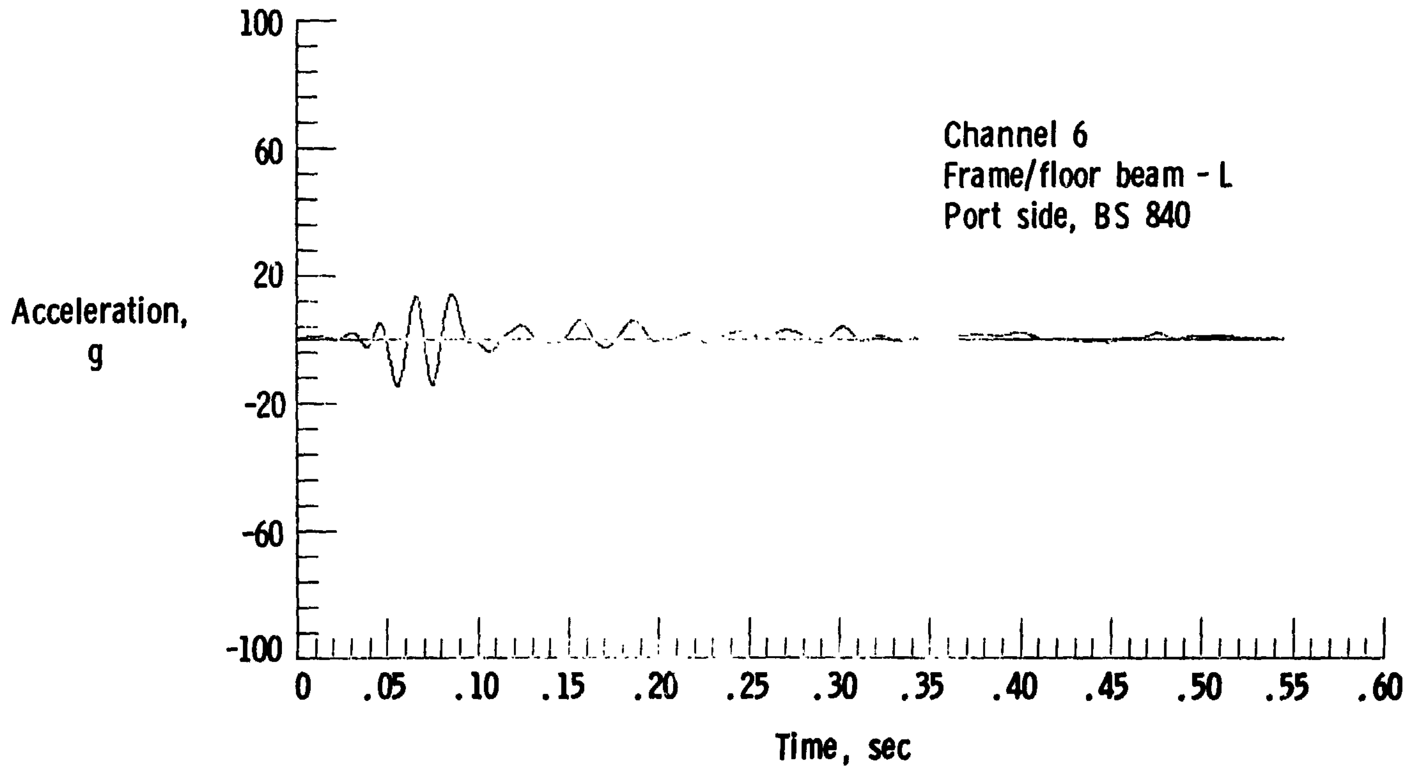

Figure 9.- Continued.

(c) Structural acceleration time histories.

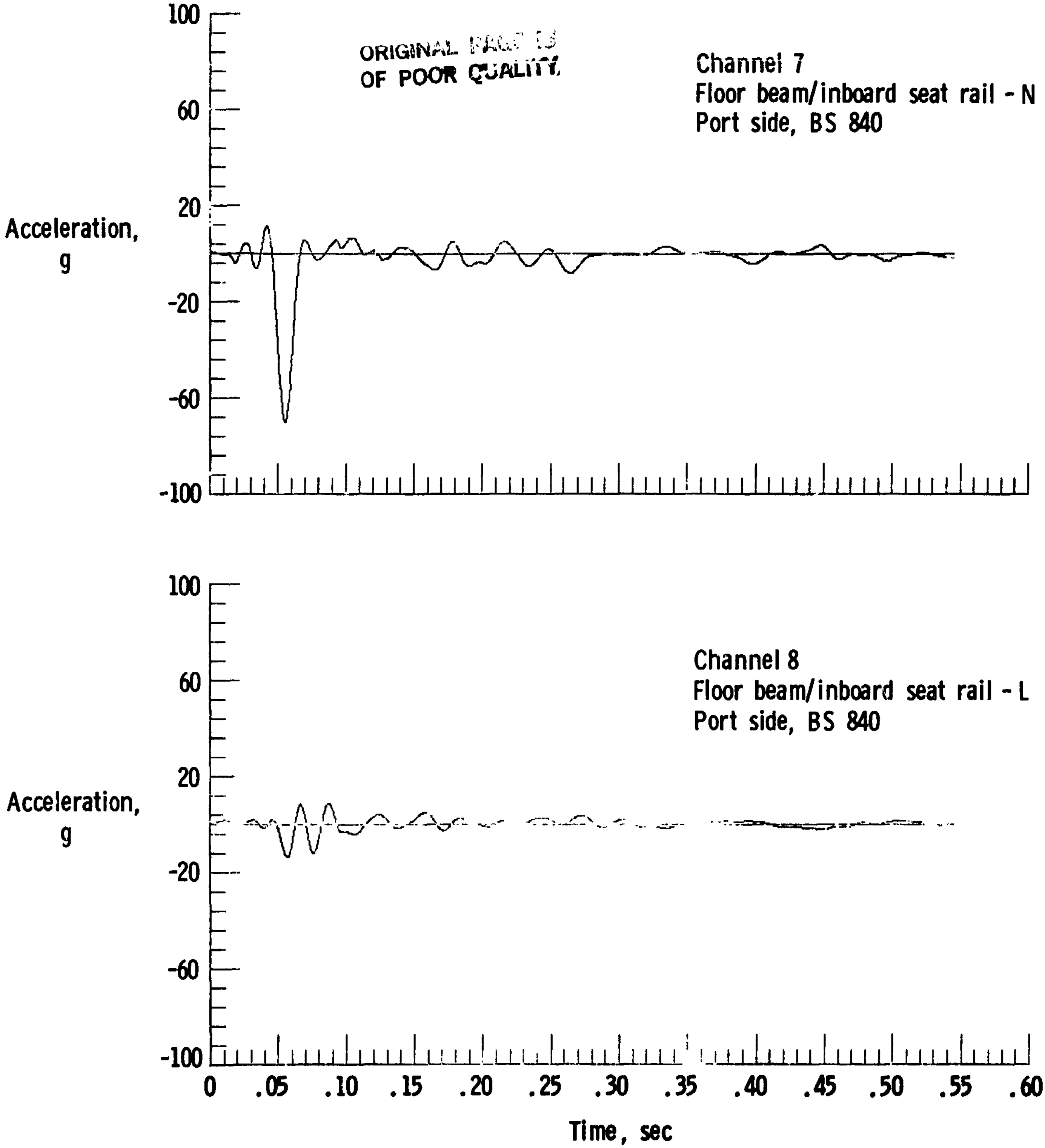

Figure 9.- Continued.

(d) Structural acceleration time histories.

ORIGINAL PAGE IS
OF POOR QUALITY

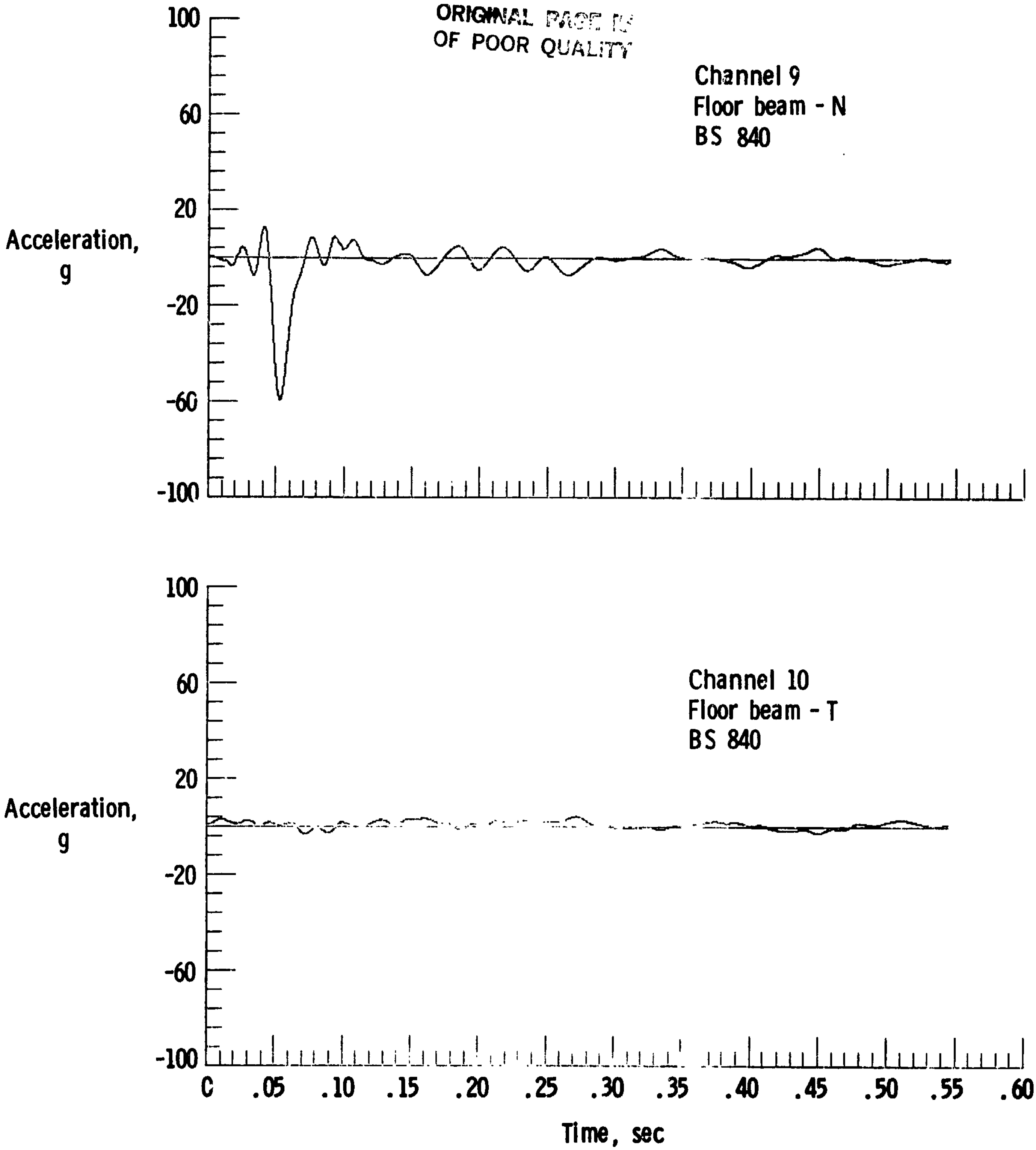

Figure 9.- Continued.

(e) Structural acceleration time histories.

ORIGINAL PAGE IS
OF POOR QUALITY

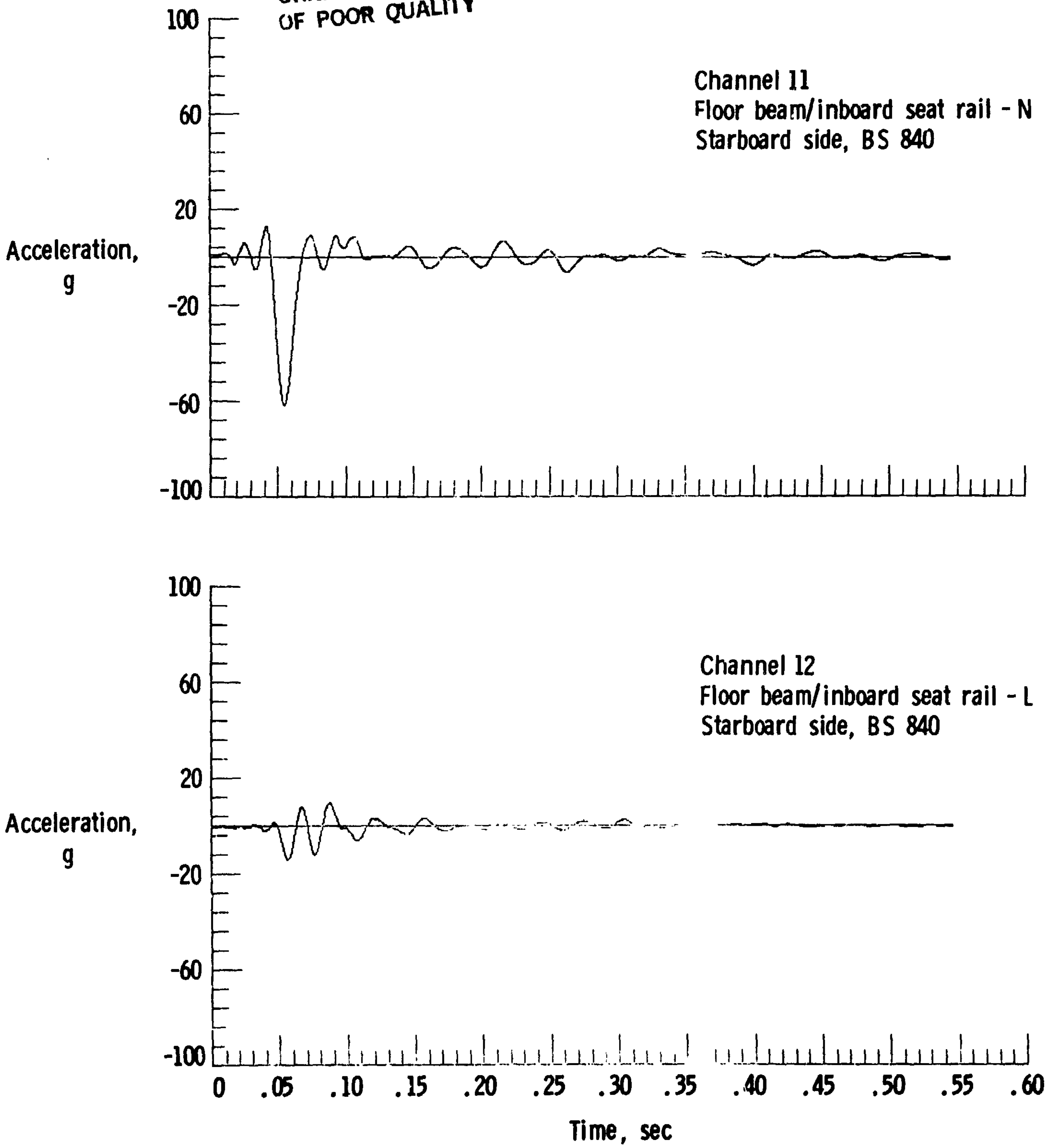

Figure 9.- Continued.

(f) Structural acceleration time histories.

ORIGINAL PAGE IS
OF POOR QUALITY

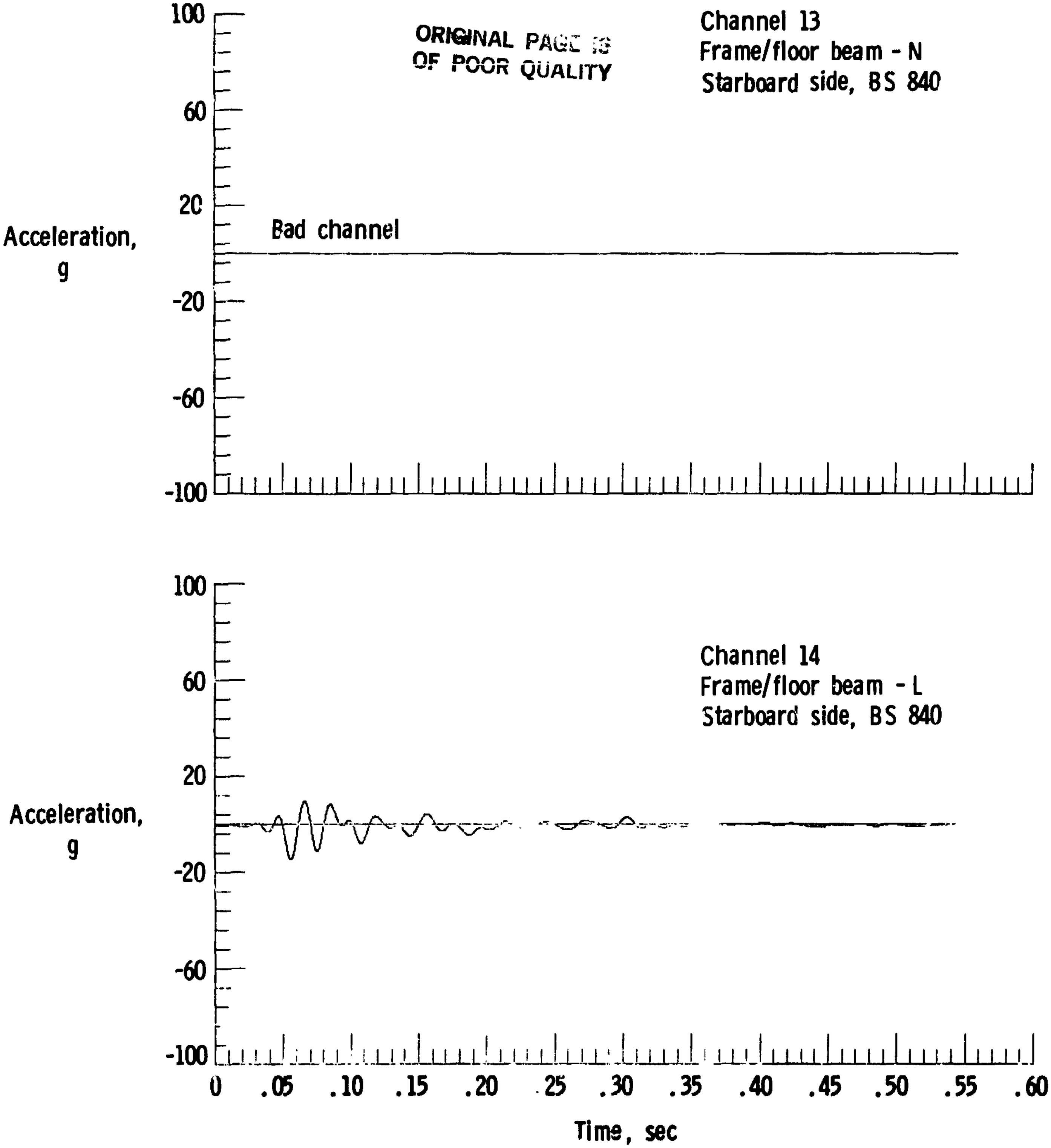

Figure 9.- Continued.

(g) Structural acceleration time histories.

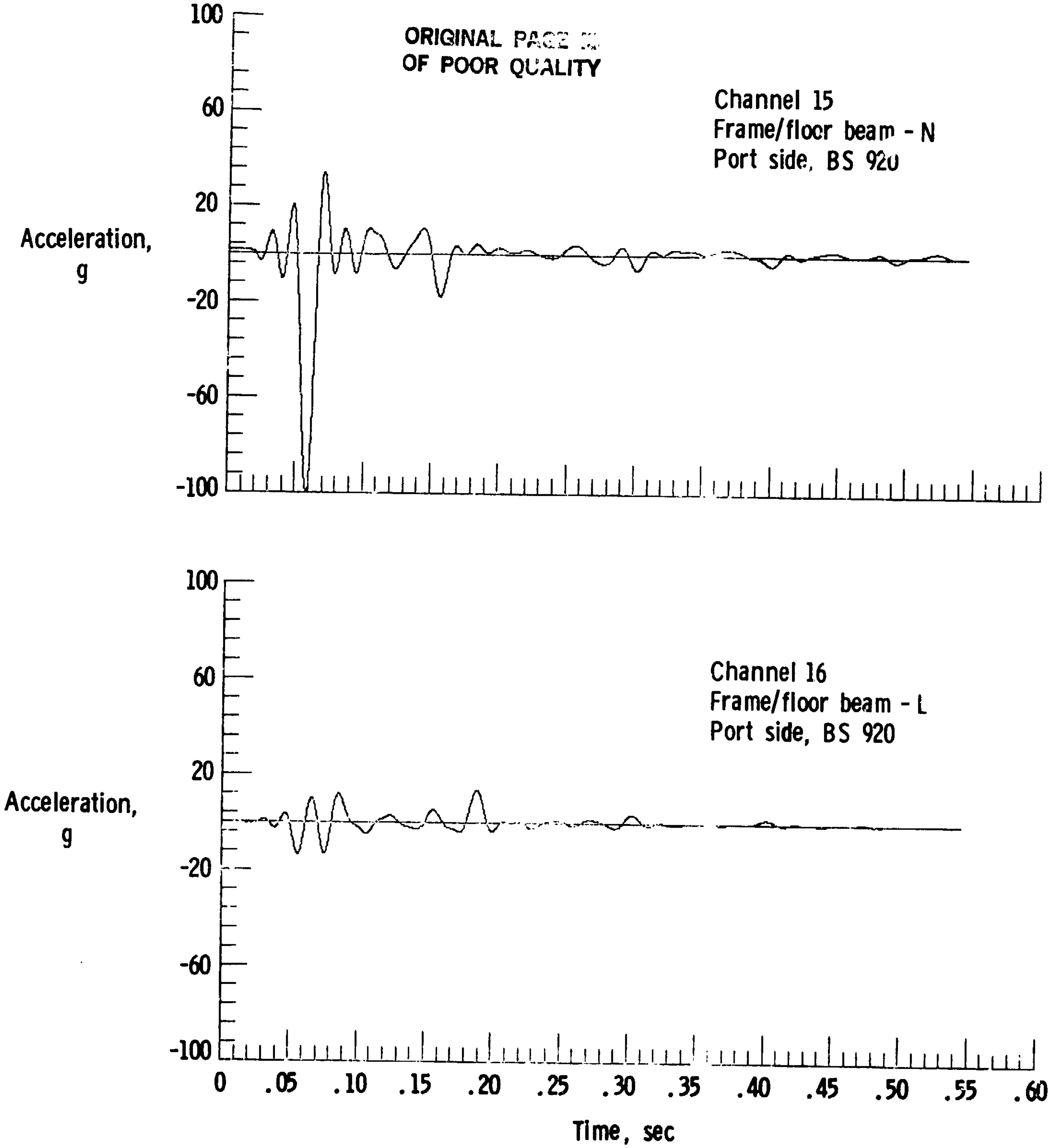

Figure 9.- Continued.

(h) Structural acceleration time histories.

ORIGINAL PAGE IS
OF POOR QUALITY

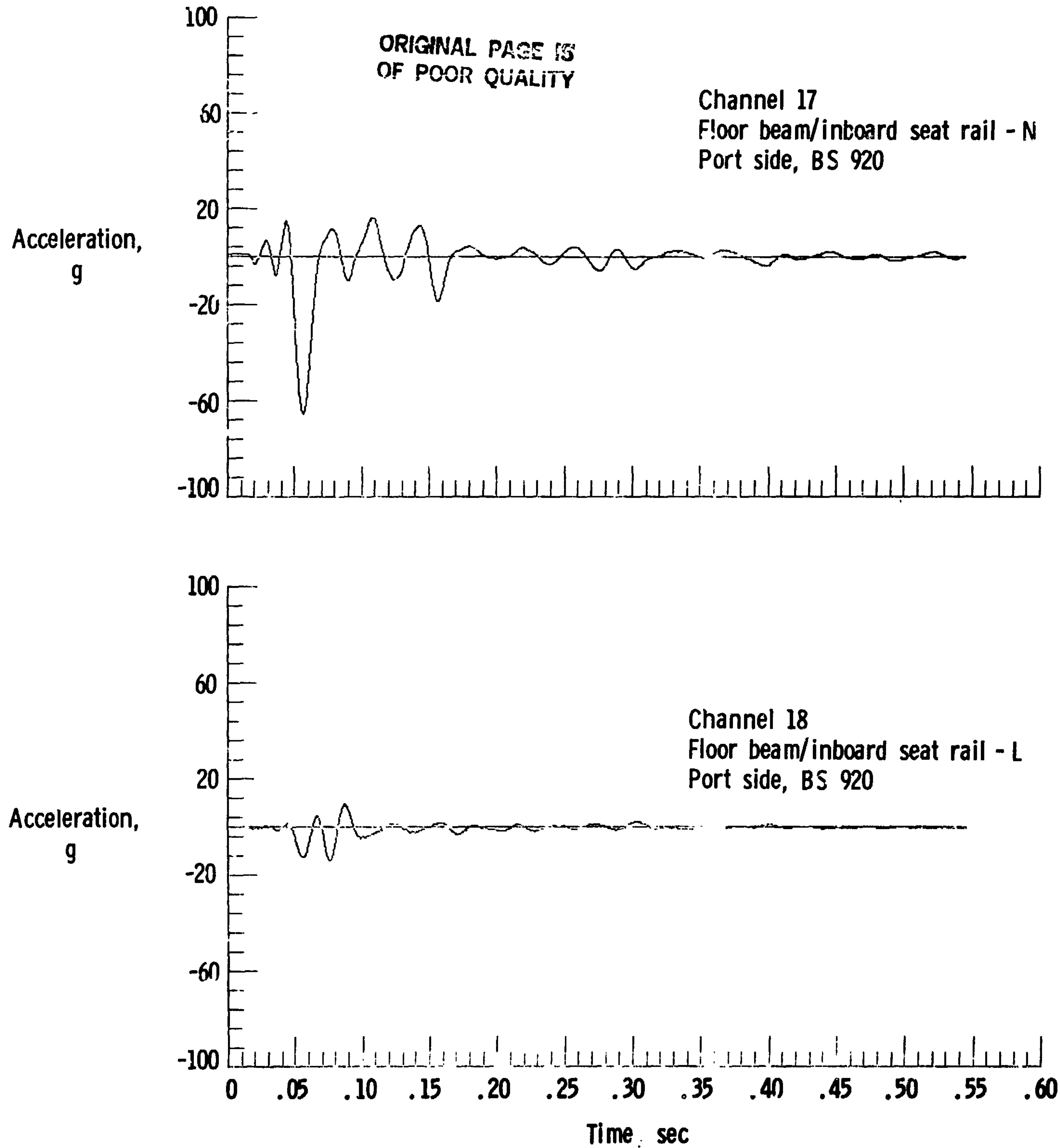

Figure 9.- Continued.

(i) Structural acceleration time histories.

ORIGINAL PAGE IS
OF POOR QUALITY

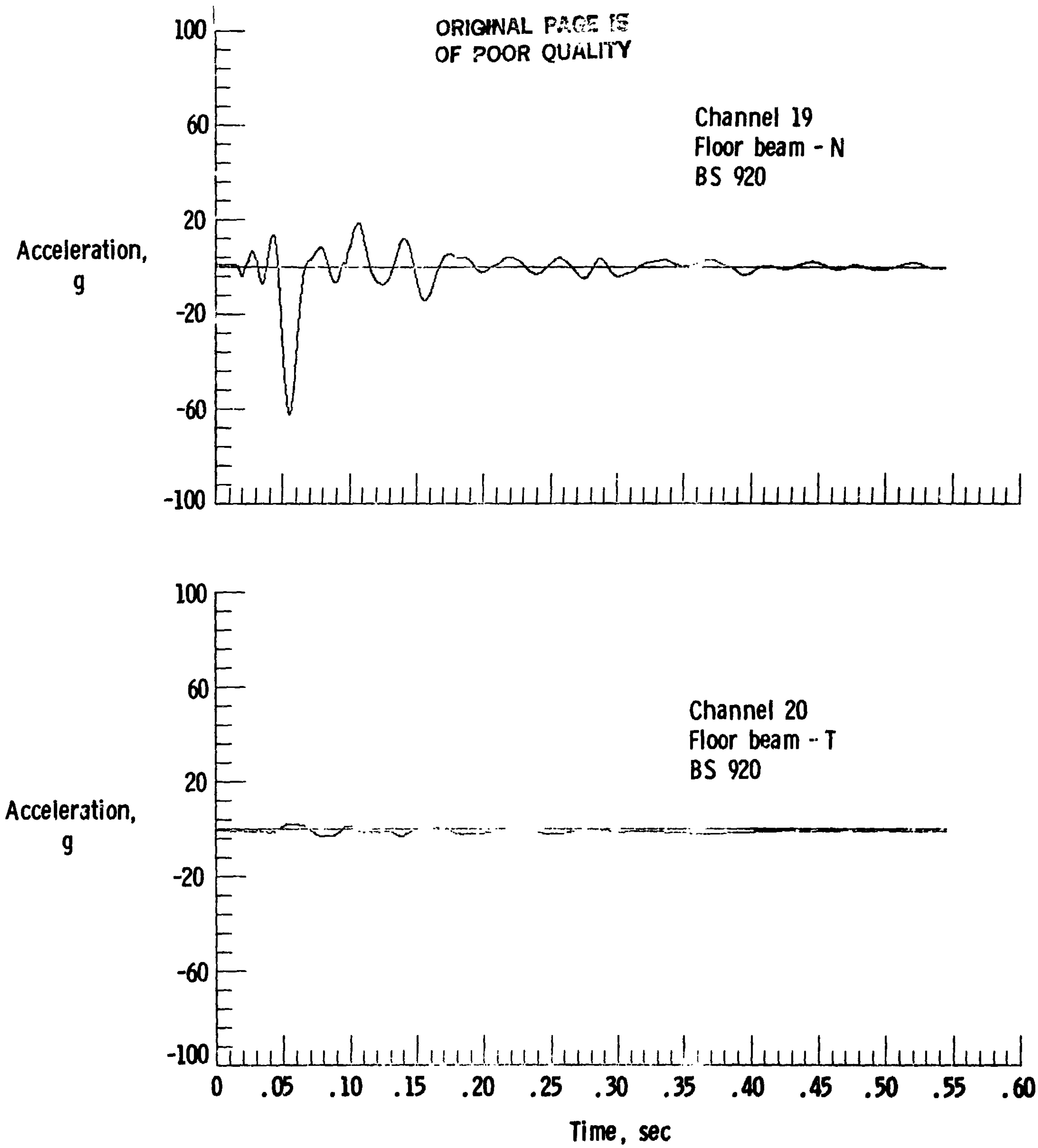

Figure 9.- Continued.

(j) Structural acceleration time histories.

ORIGINAL PAGE IS
OF POOR QUALITY

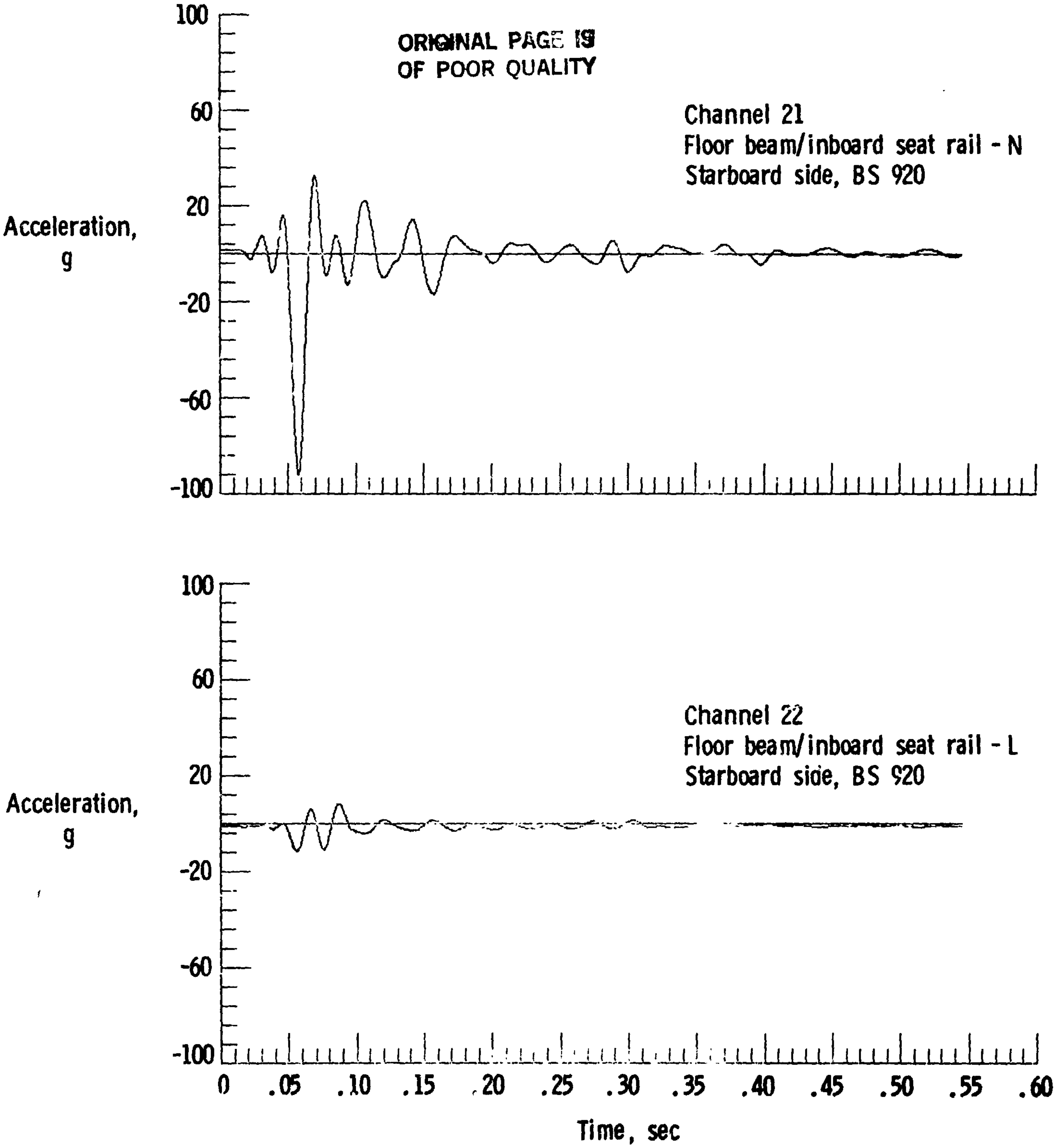

Figure 9.- Continued.

(k) Structural acceleration time histories.

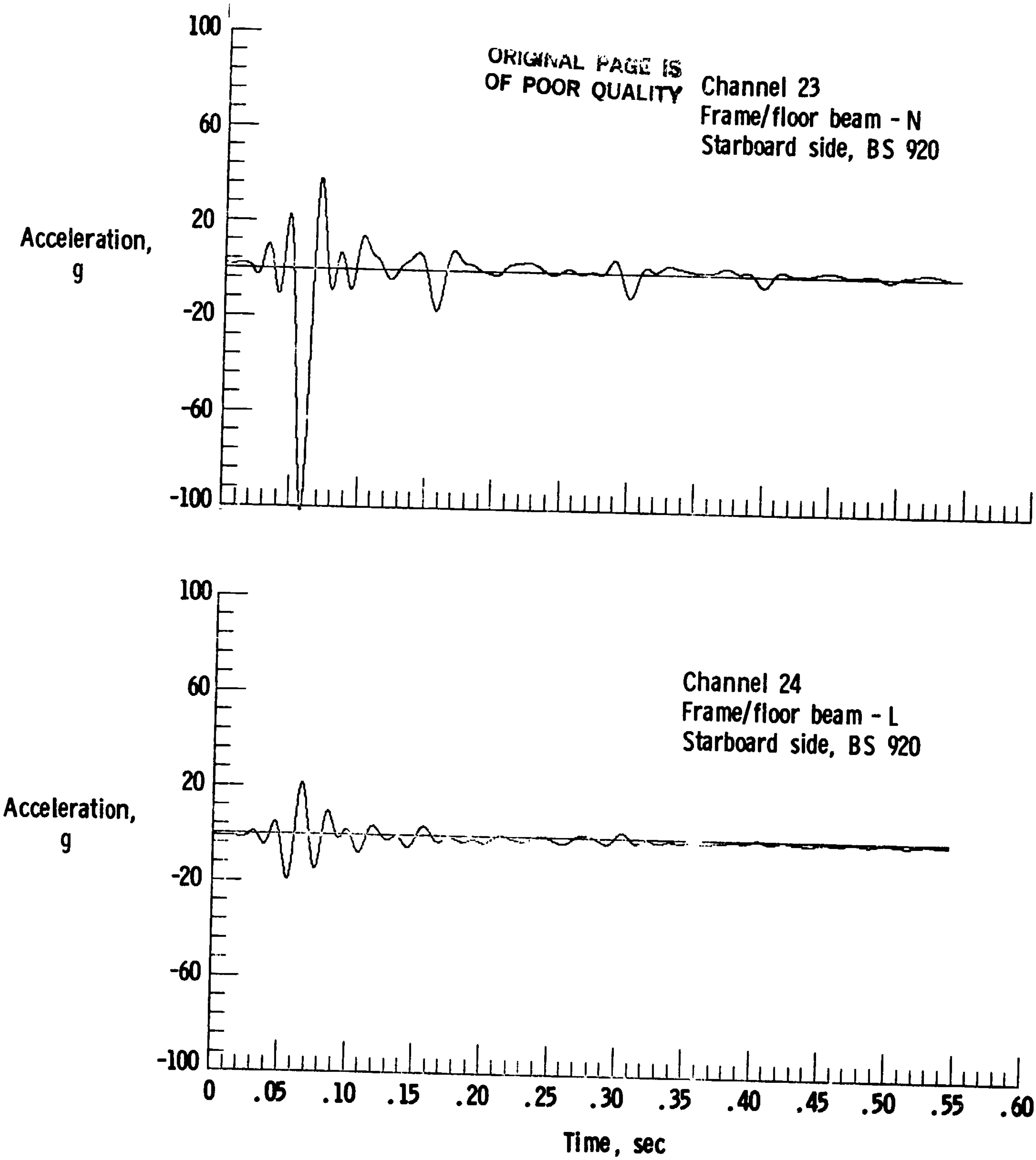

Figure 9.- Continued.

(l) Structural acceleration time histories.

ORIGINAL PAGE IS
OF POOR QUALITY

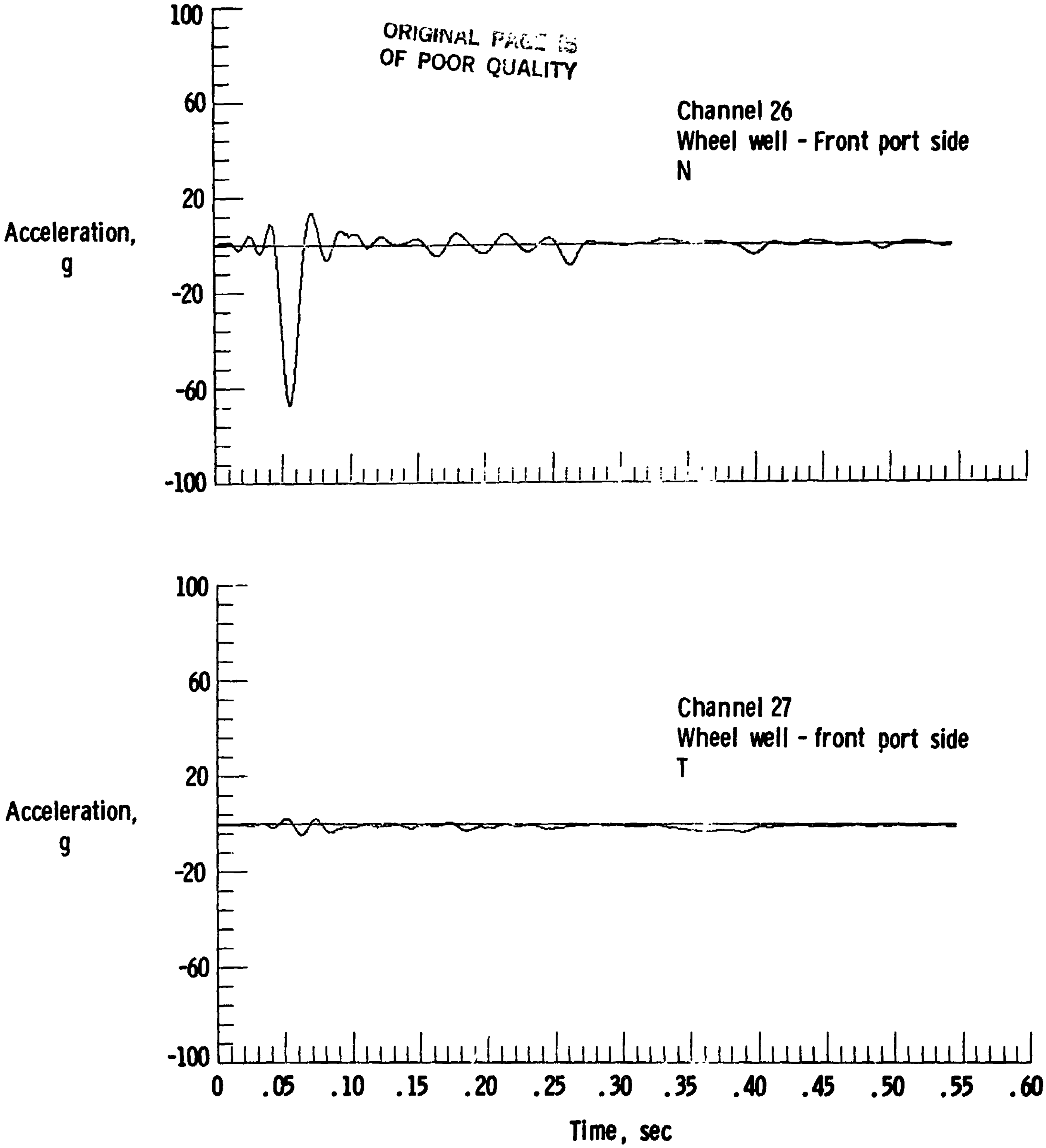

Figure 9.- Continued.

(m) Structural acceleration time histories.

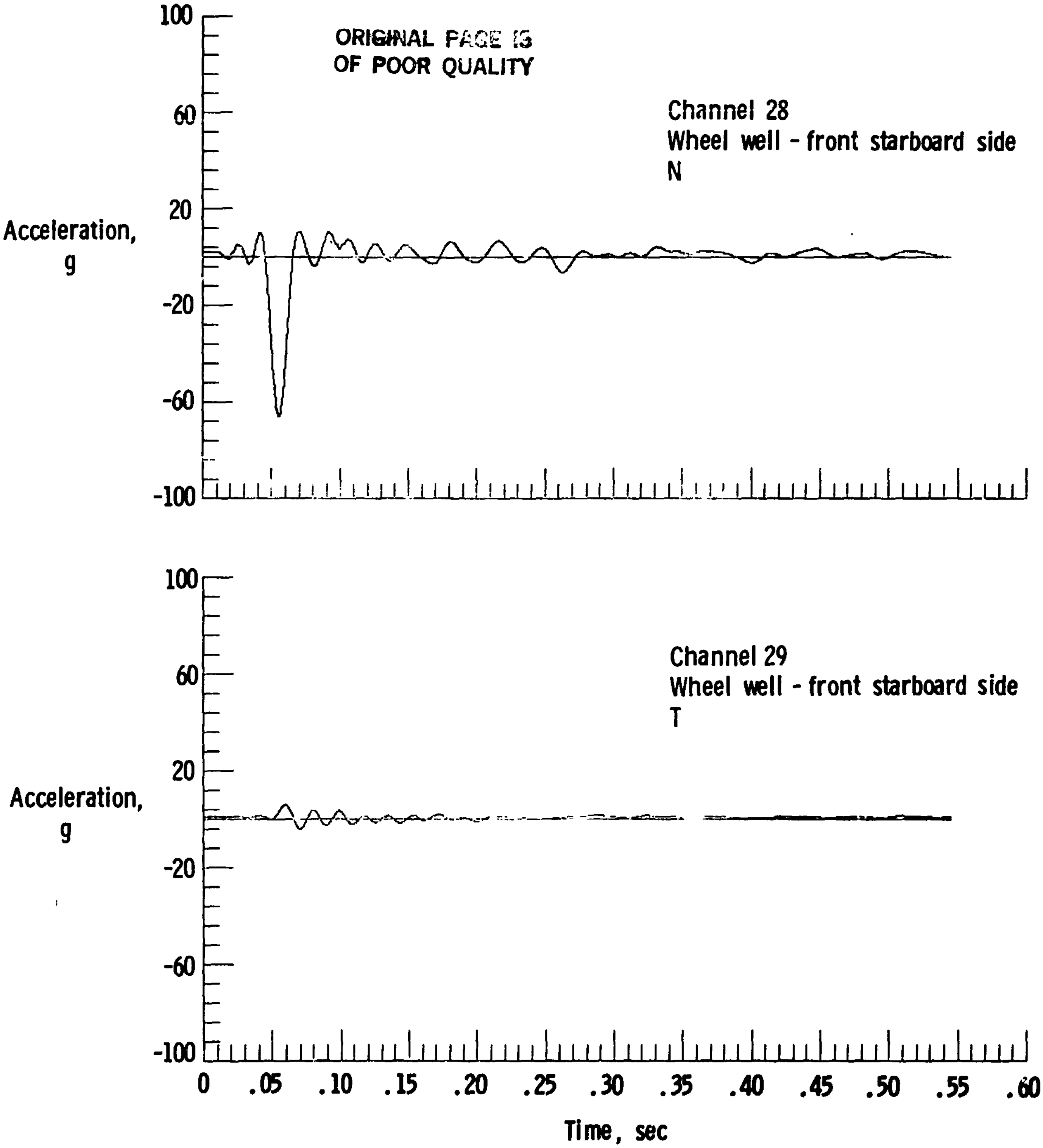

Figure 9.- Continued.

(n) Structural acceleration time histories.

ORIGINAL PAGE IS
OF POOR QUALITY

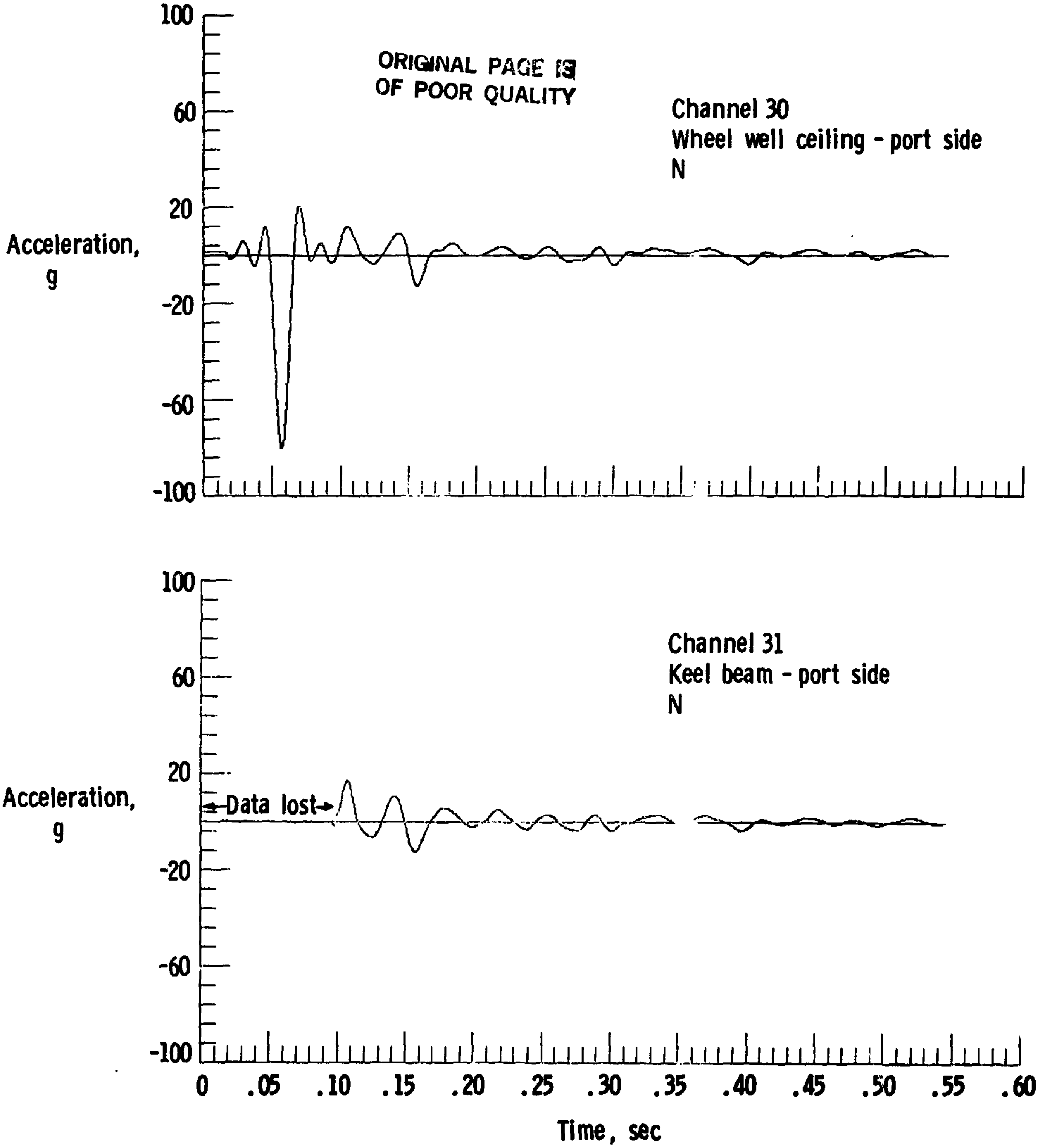

Figure 9.- Continued.

(o) Structural acceleration time histories.

ORIGINAL PAGE IS
OF POOR QUALITY

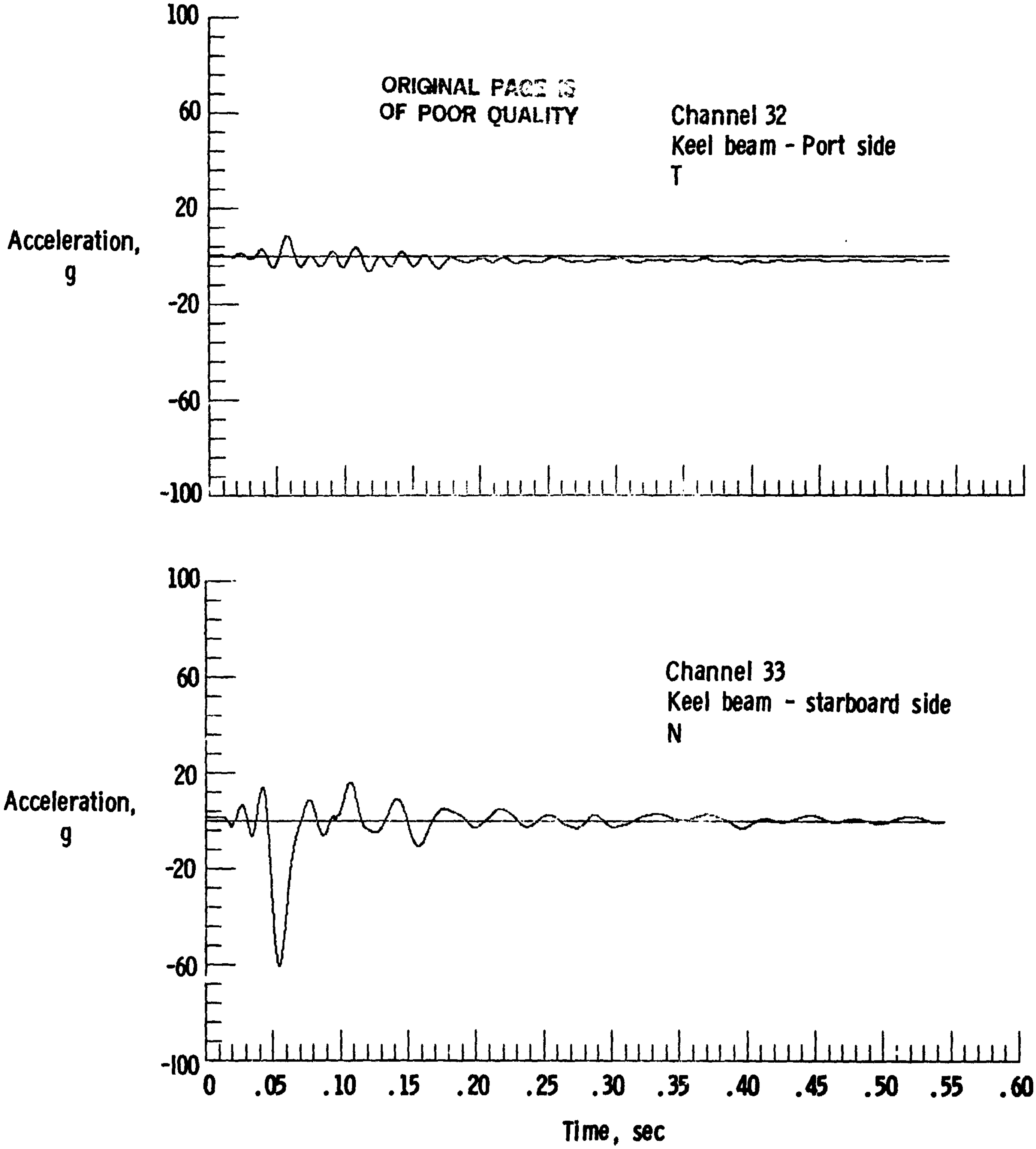

Figure 9.- Continued.

(p) Structural acceleration time histories.

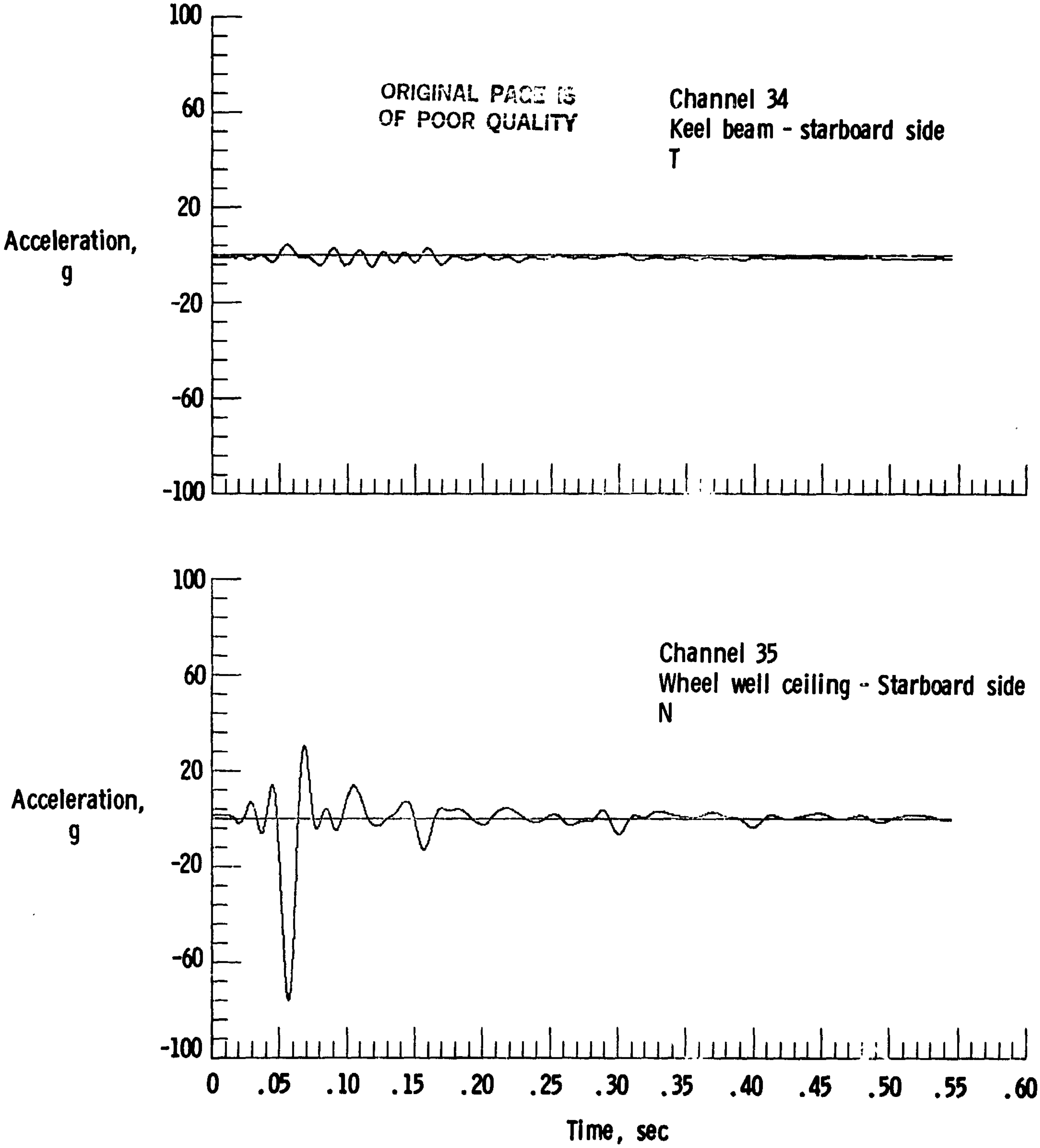

ORIGINAL PAGE IS
OF POOR QUALITY

Figure 9.- Continued.

(q) Structural acceleration time histories.

ORIGINAL PAGE IS
OF POOR QUALITY

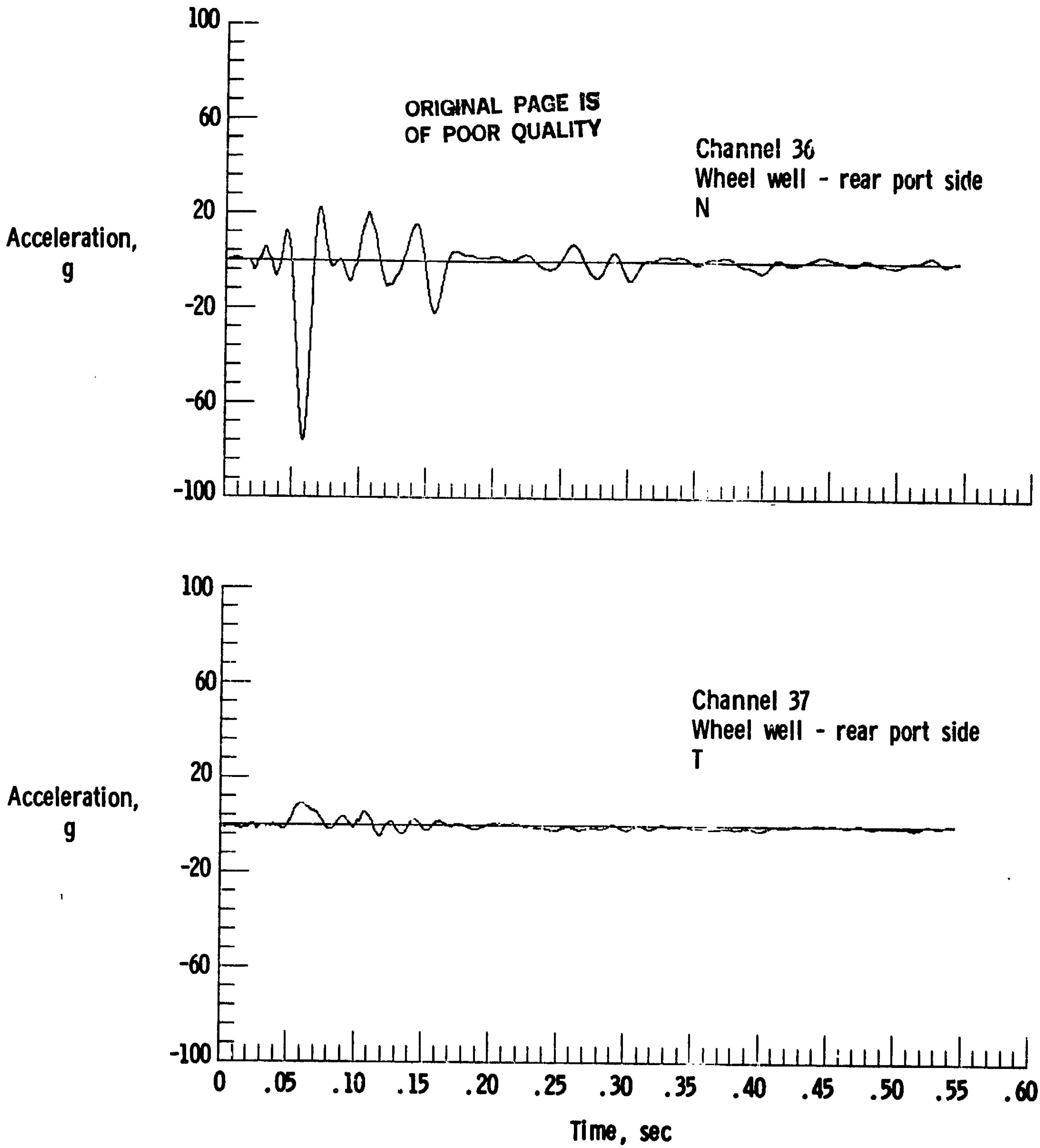

Figure 9.- Continued.

(r) Structural acceleration time histories.

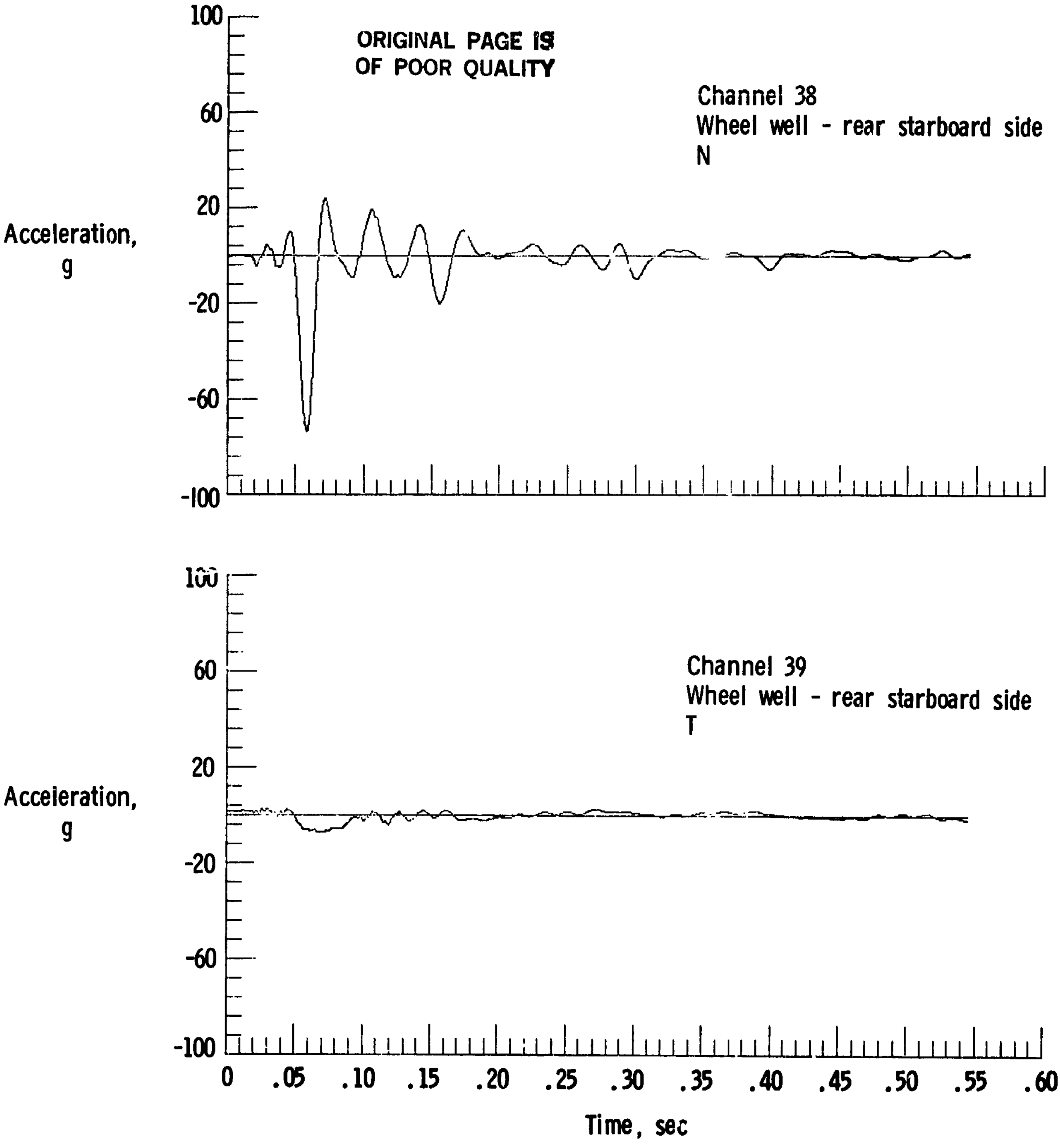

Figure 9.- Concluded.

(s) Structural acceleration time histories.

ORIGINAL PAGE IS
OF POOR QUALITY

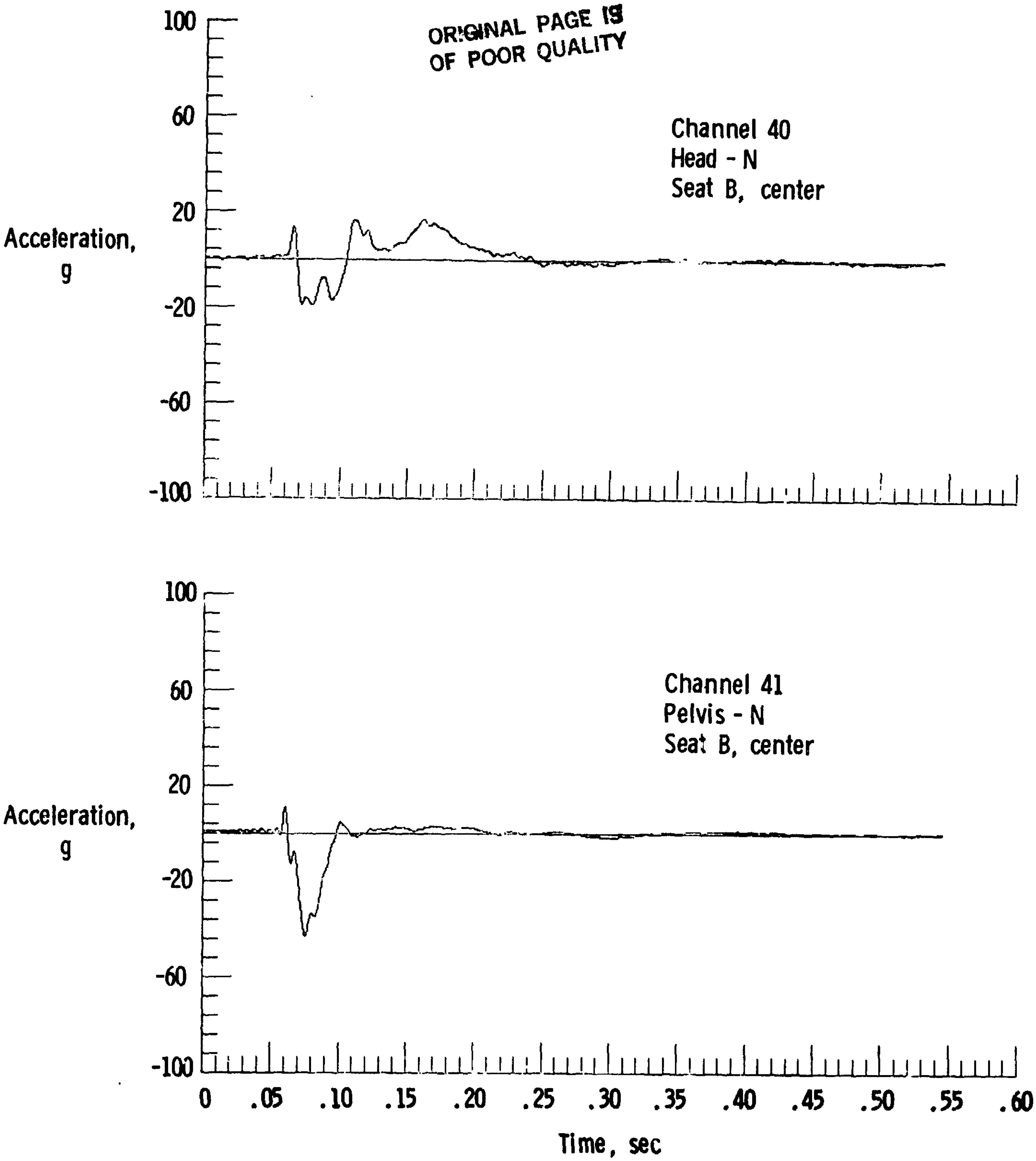

(a) Occupant accelerations.

Figure 10.- Acceleration time histories measured in anthropomorphic dummies.

ORIGINAL PAGE IS
OF POOR QUALITY

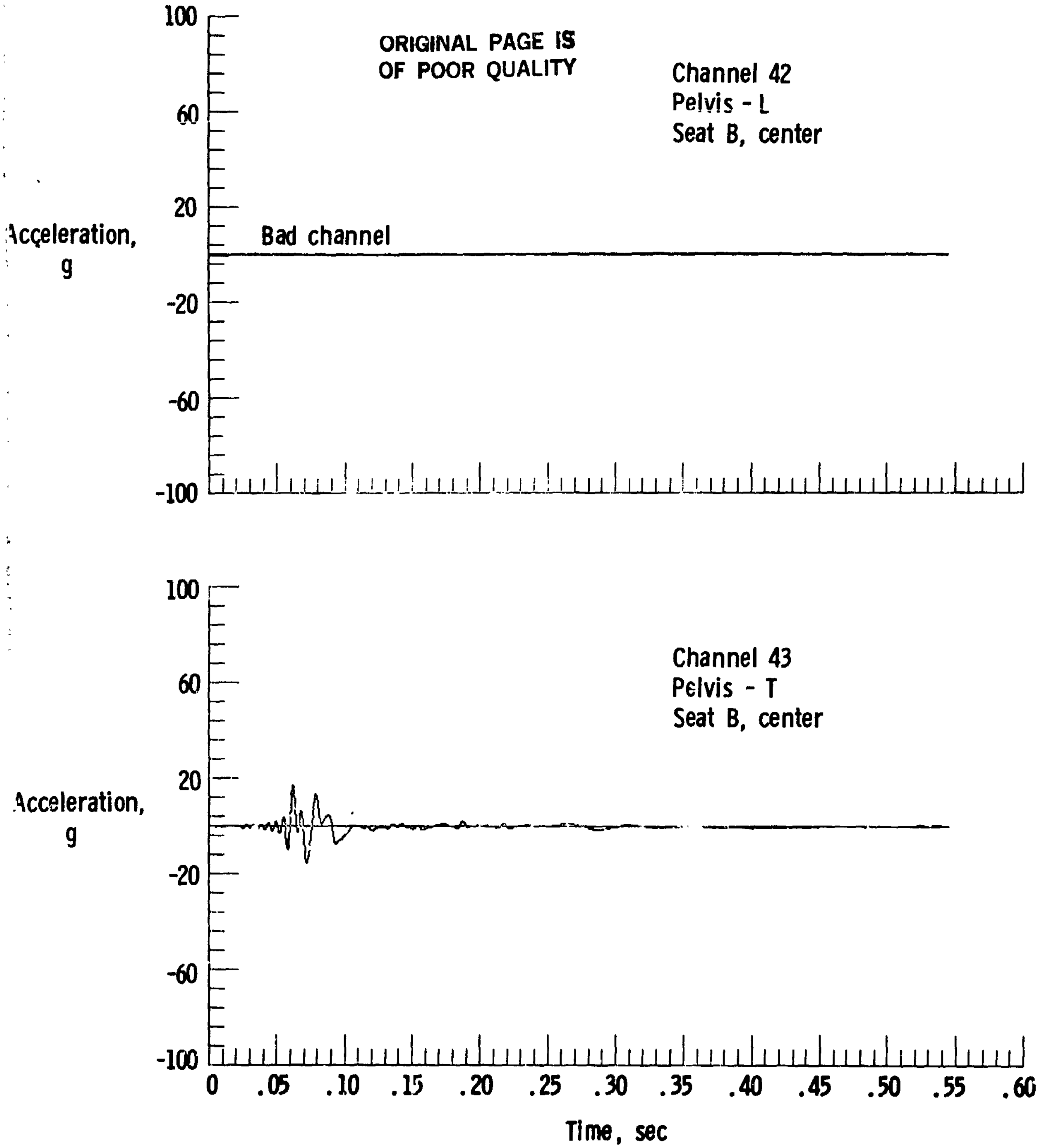

Figure 10.- Continued.

(b) Occupant accelerations.

ORIGINAL PAGE IS
OF POOR QUALITY

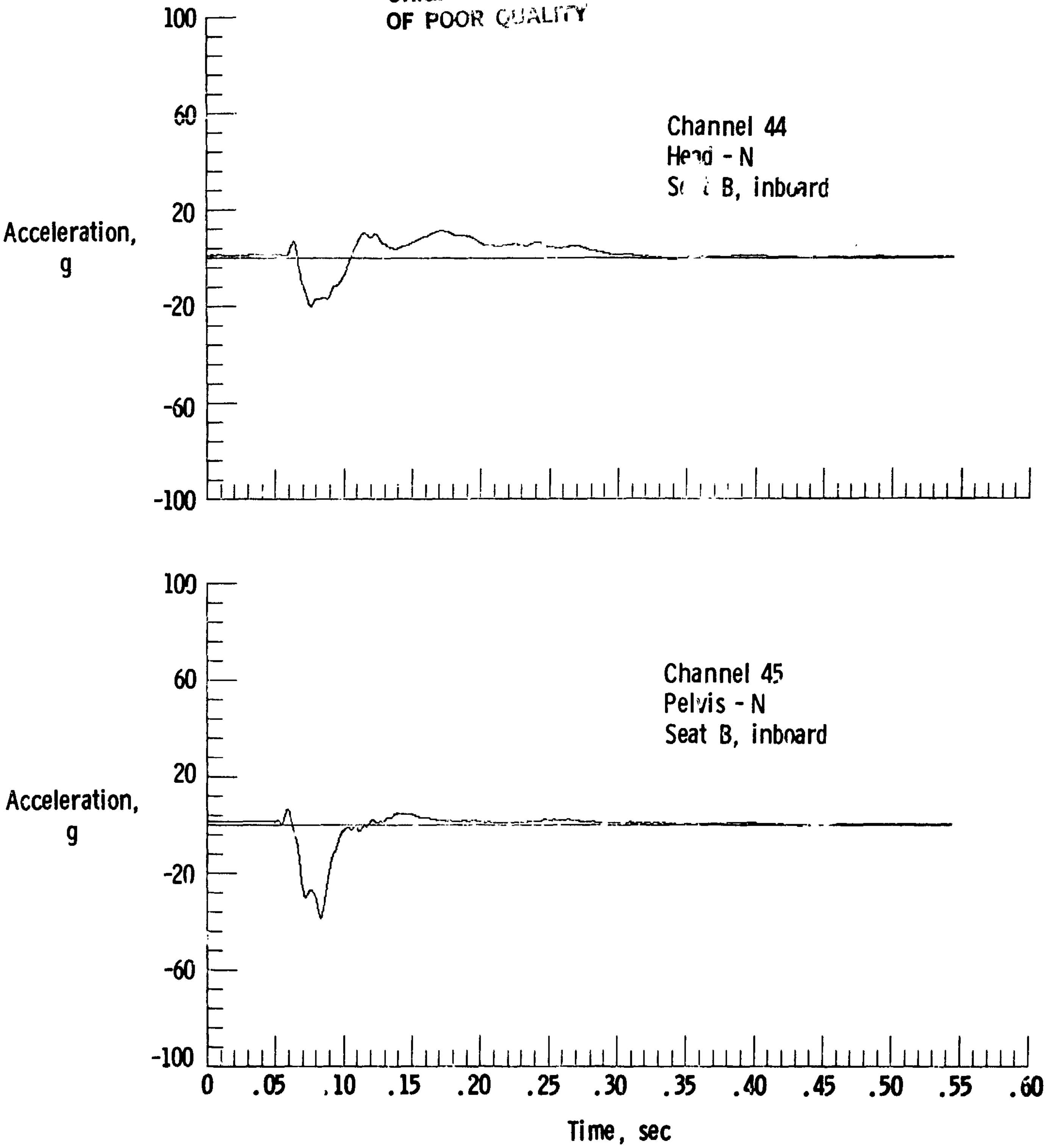

Figure 10.- Continued.

(c) Occupant accelerations.

ORIGINAL PAGE IS
OF POOR QUALITY

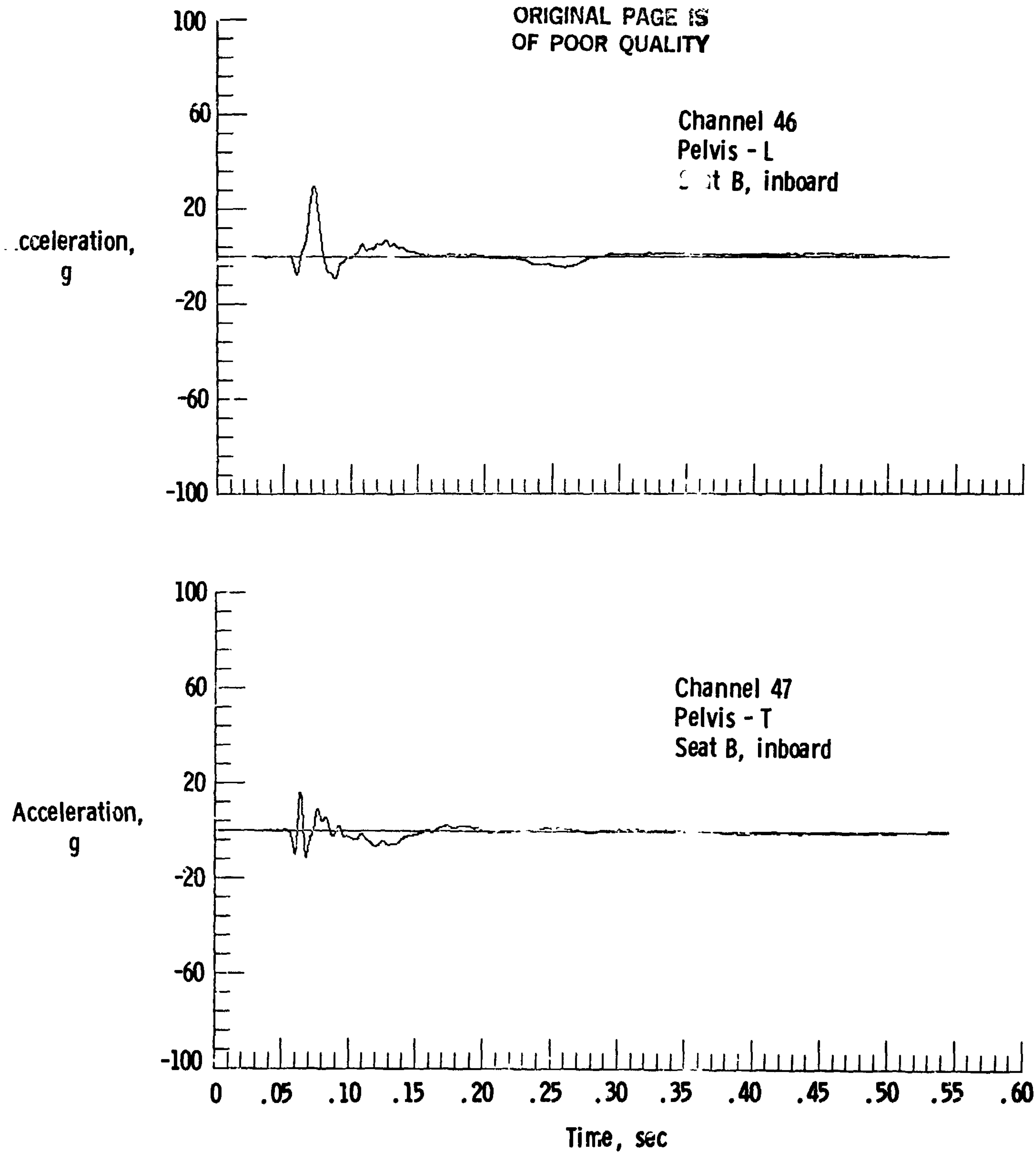

Figure 10.- Continued.

(d) Occupant accelerations.

ORIGINAL PAGE IS
OF POOR QUALITY

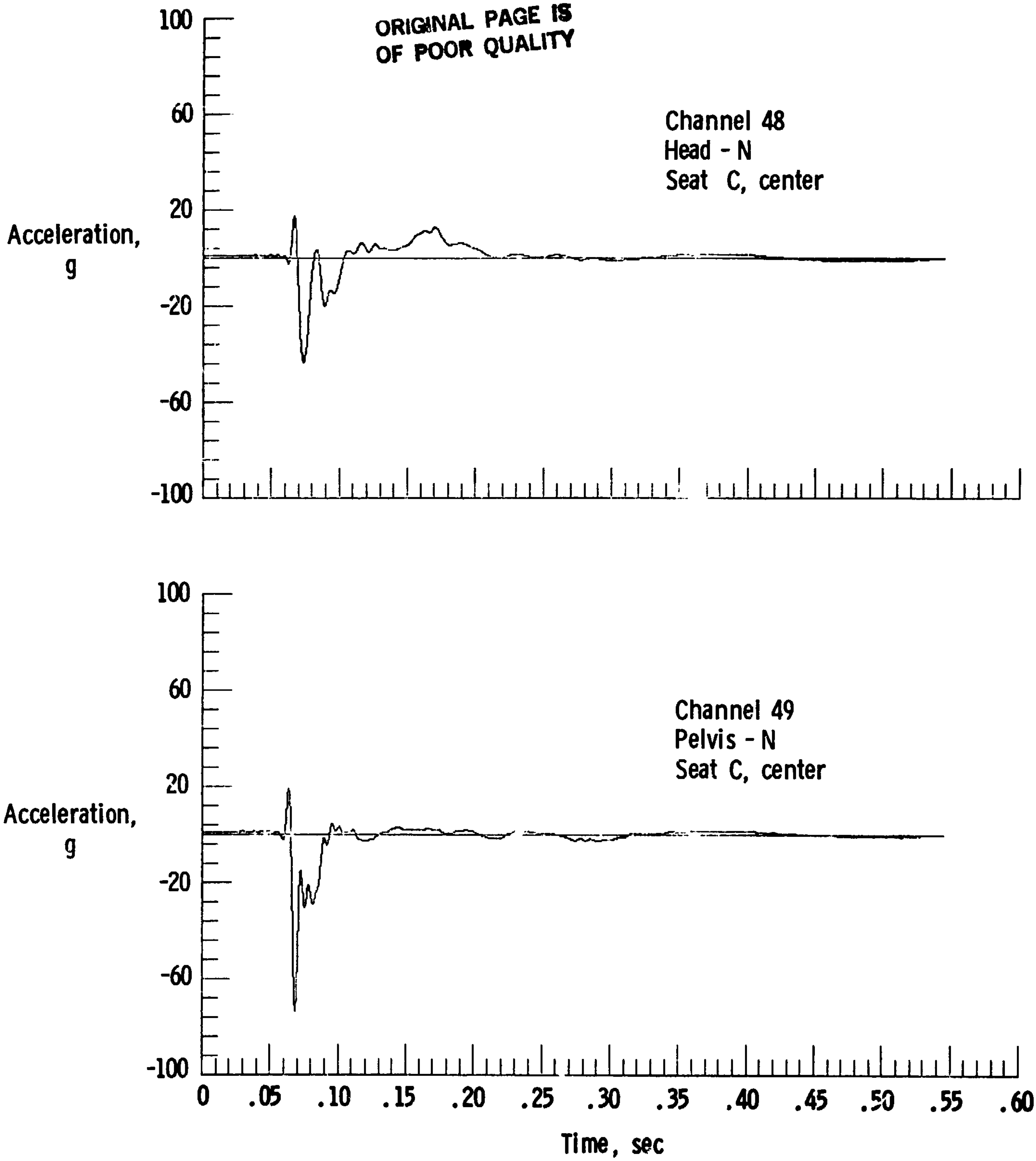

Figure 10.- Continued.

(e) Occupant accelerations.

ORIGINAL PAGE IS
OF POOR QUALITY

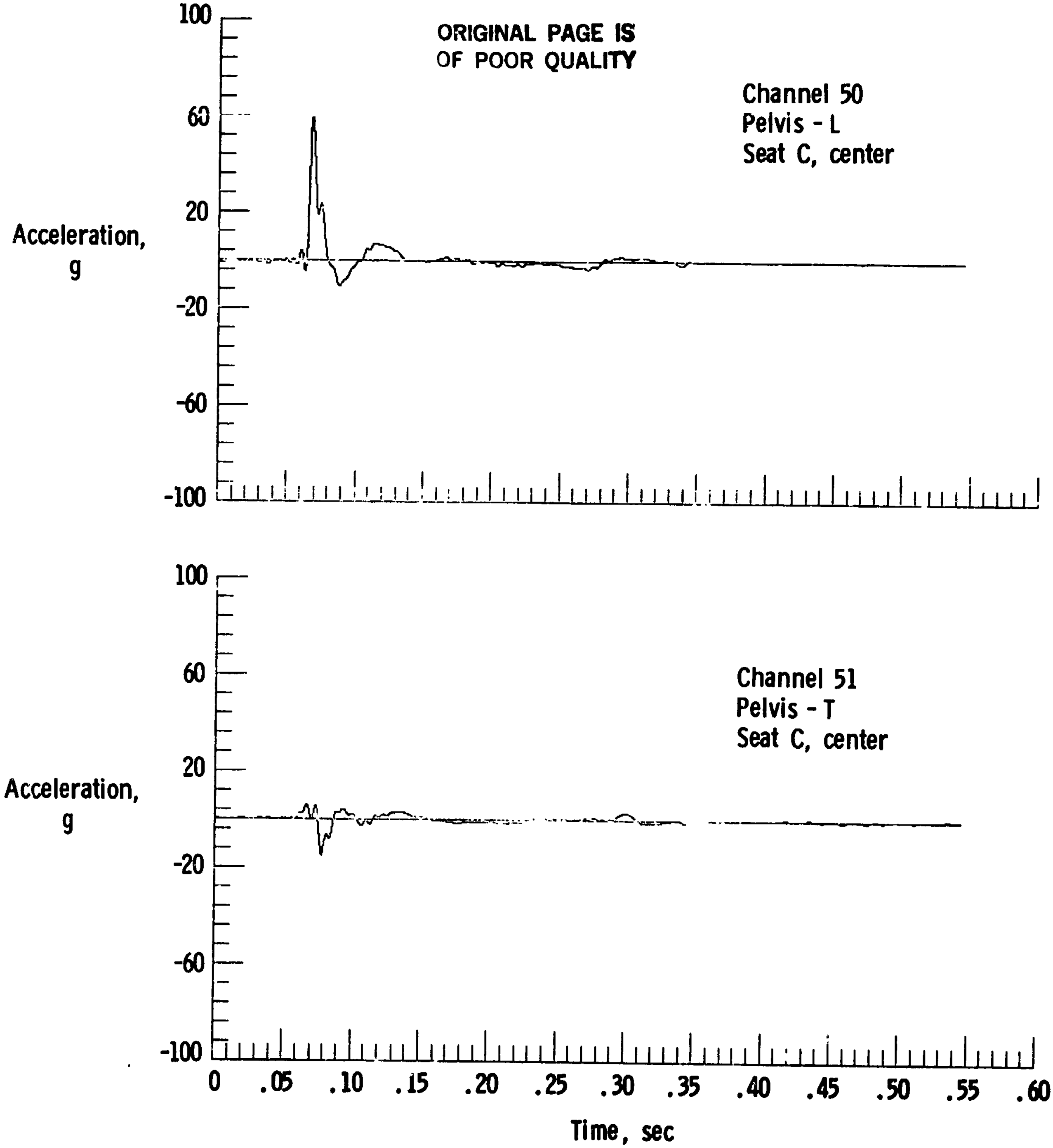

Figure 10.- Continued.

(f) Occupant accelerations.

ORIGINAL PAGE IS
OF POOR QUALITY

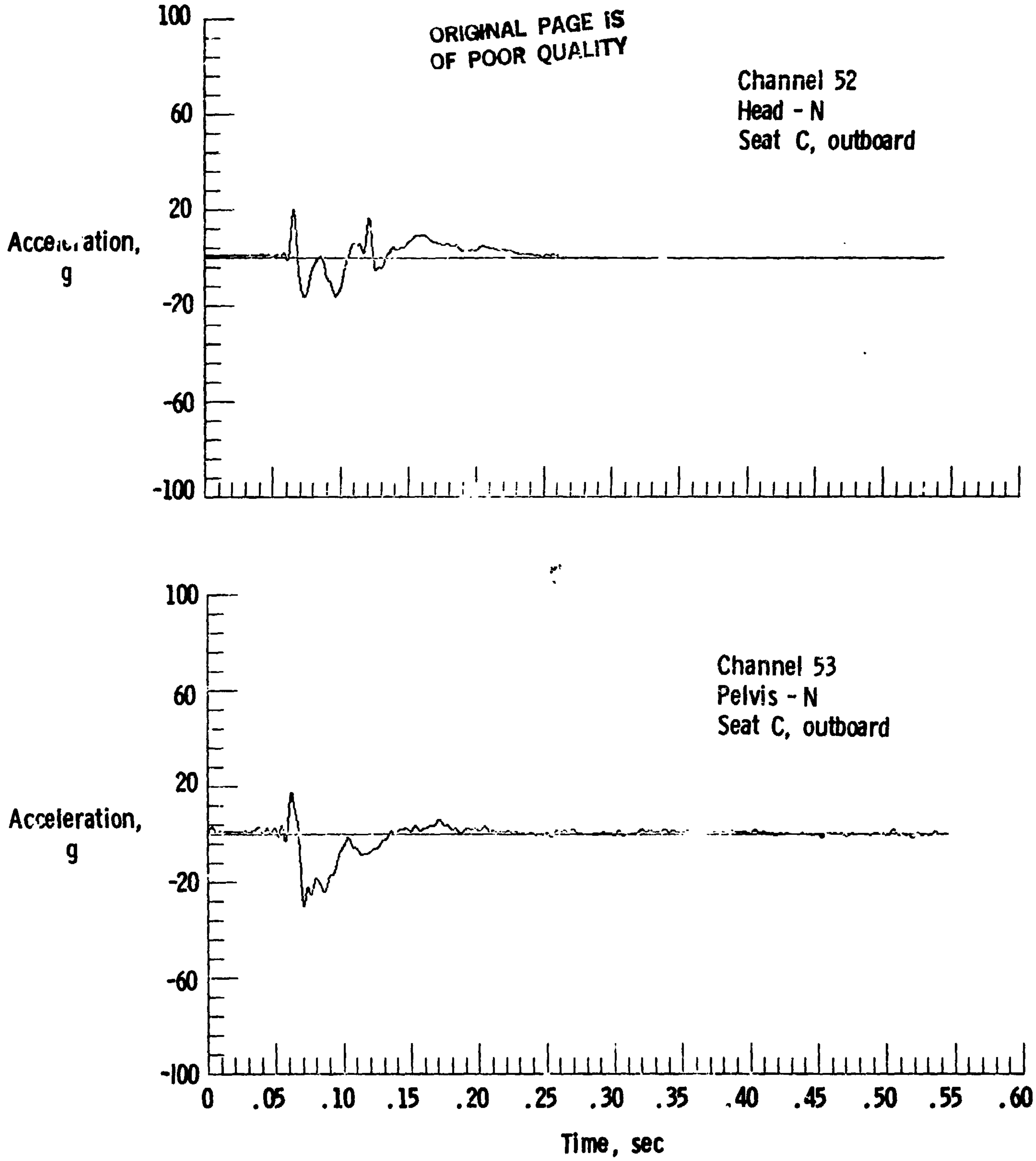

Figure 10.- Continued.

(g) Occupant accelerations.

ORIGINAL PAGE IS
OF POOR QUALITY

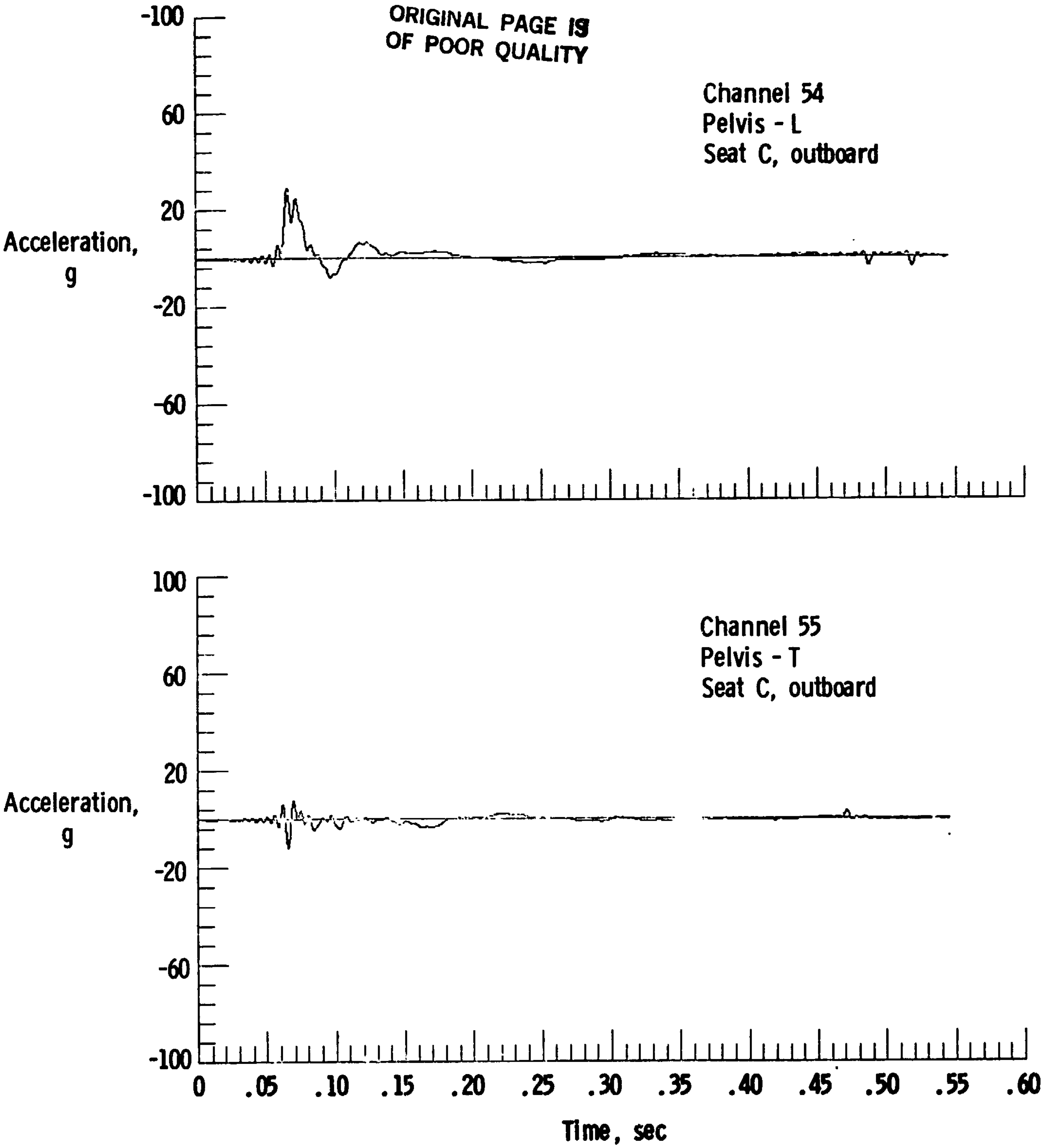

Figure 10.- Continued.

(h) Occupant accelerations.

ORIGINAL PAGE IS
OF POOR QUALITY

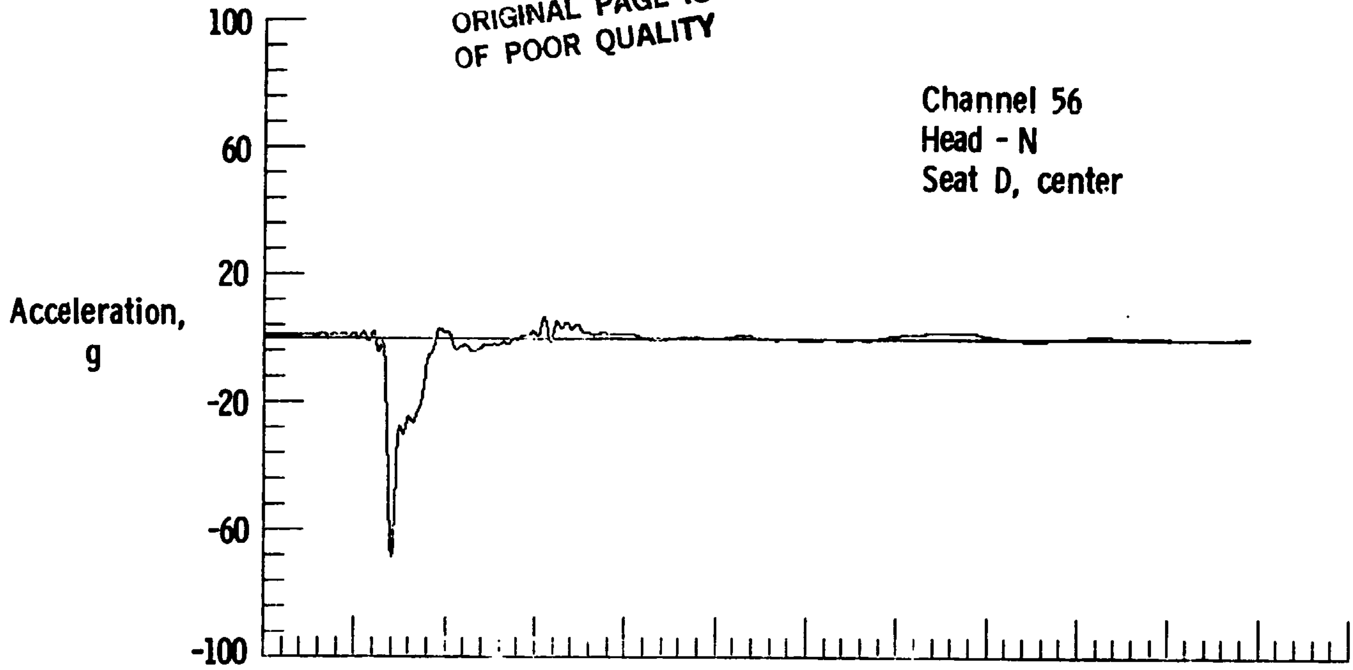

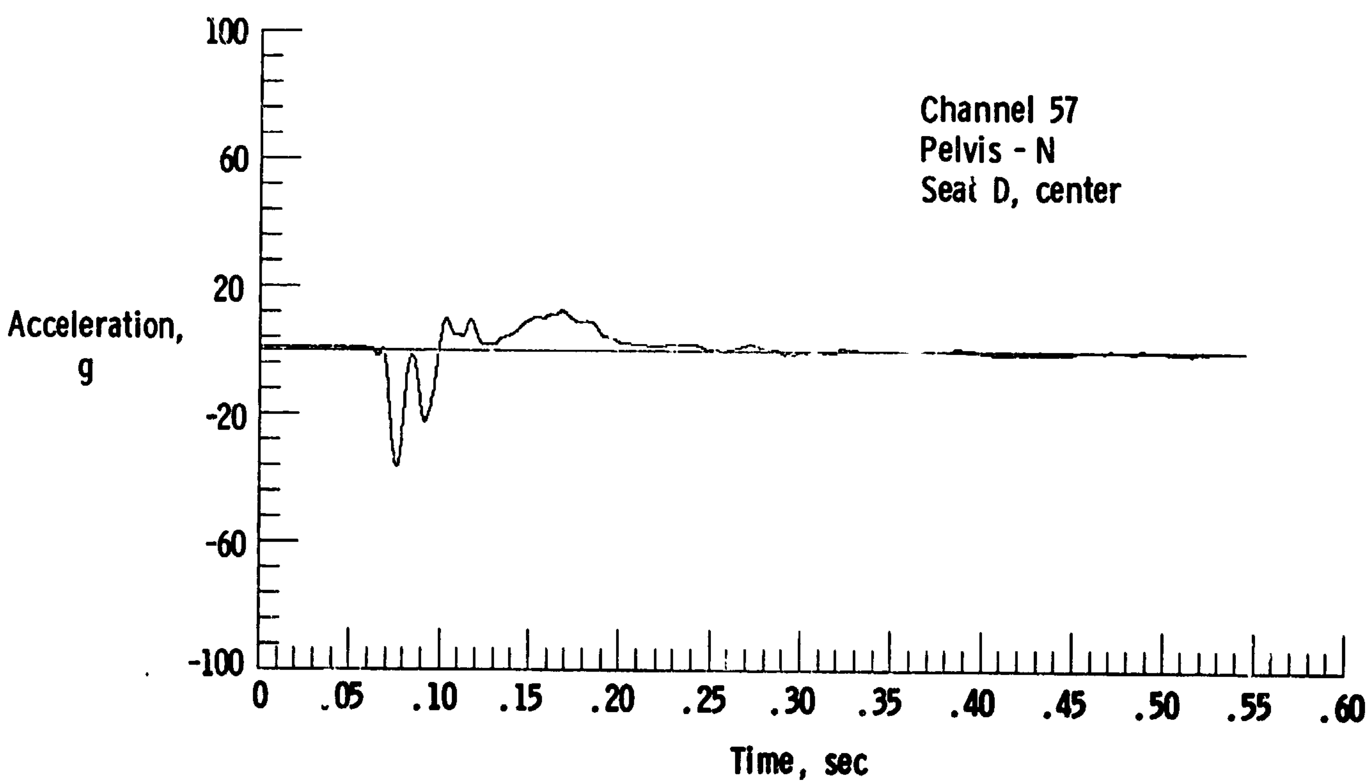

Figure 10.- Continued.

(i) Occupant accelerations.

ORIGINAL PAGE IS
OF POOR QUALITY

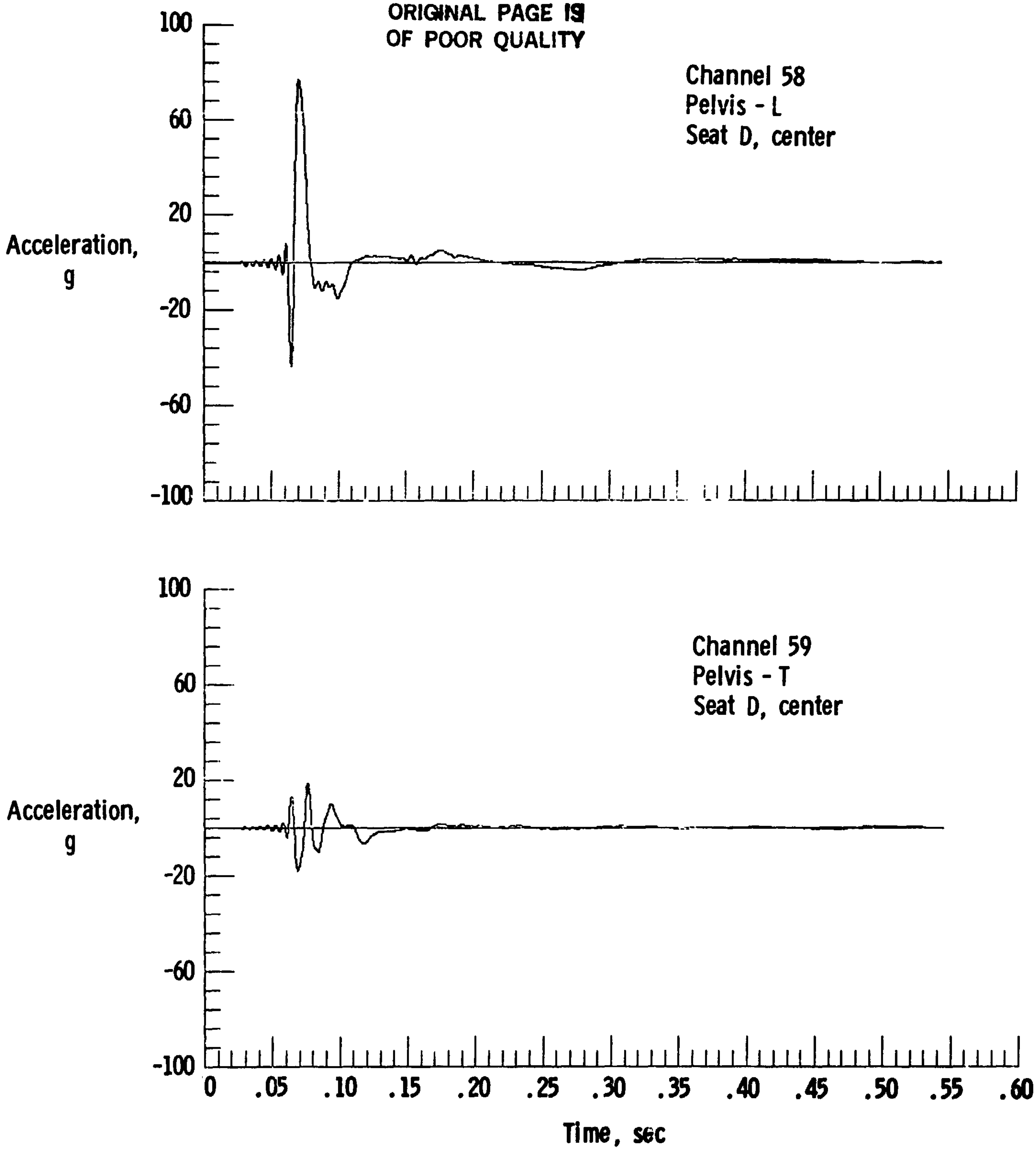

Figure 10.- Continued.

(j) Occupant accelerations.

ORIGINAL PAGE IS
OF POOR QUALITY

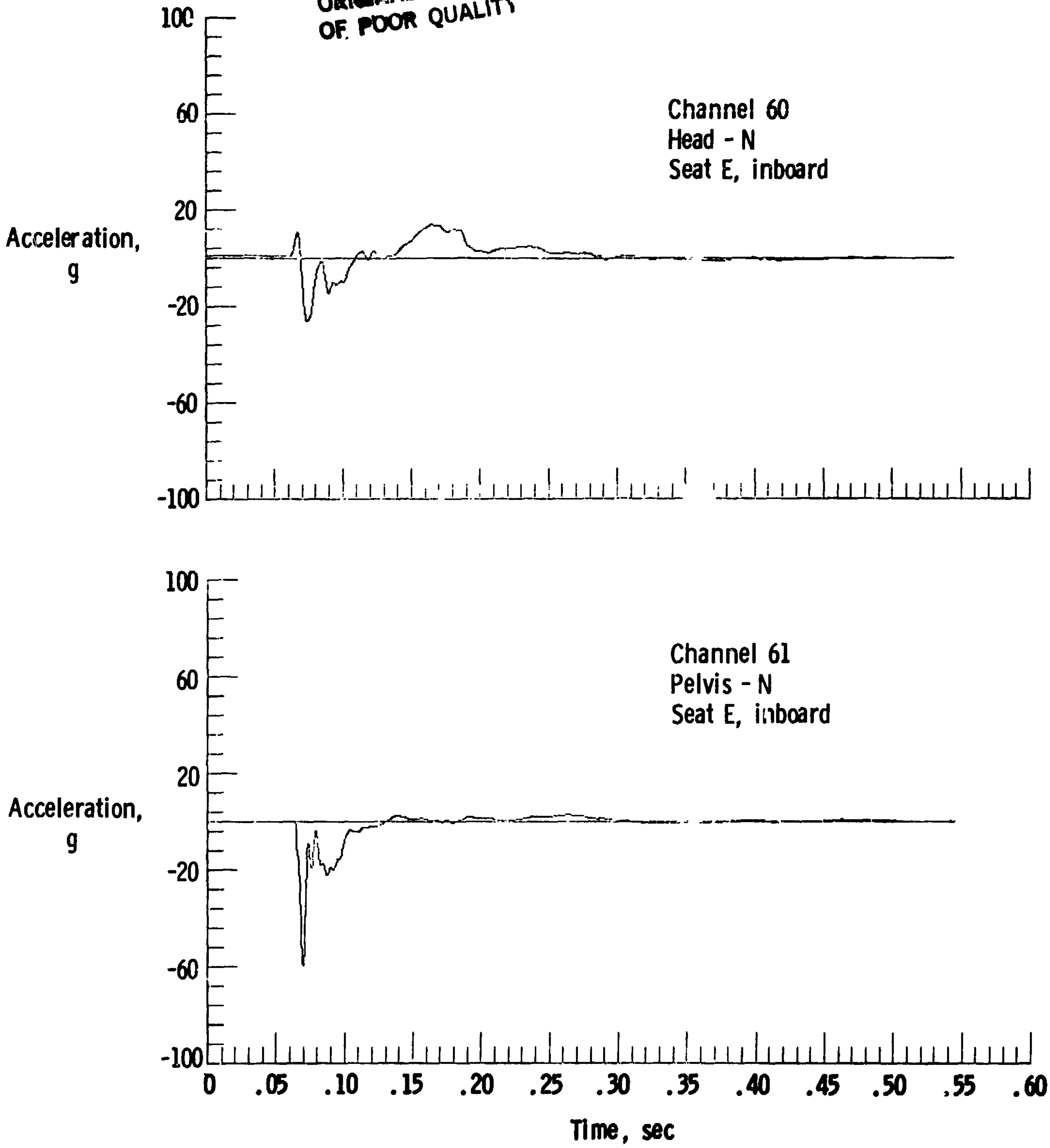

Figure 10.- Continued.

(k) Occupant accelerations.

ORIGINAL PAGE IS
OF POOR QUALITY

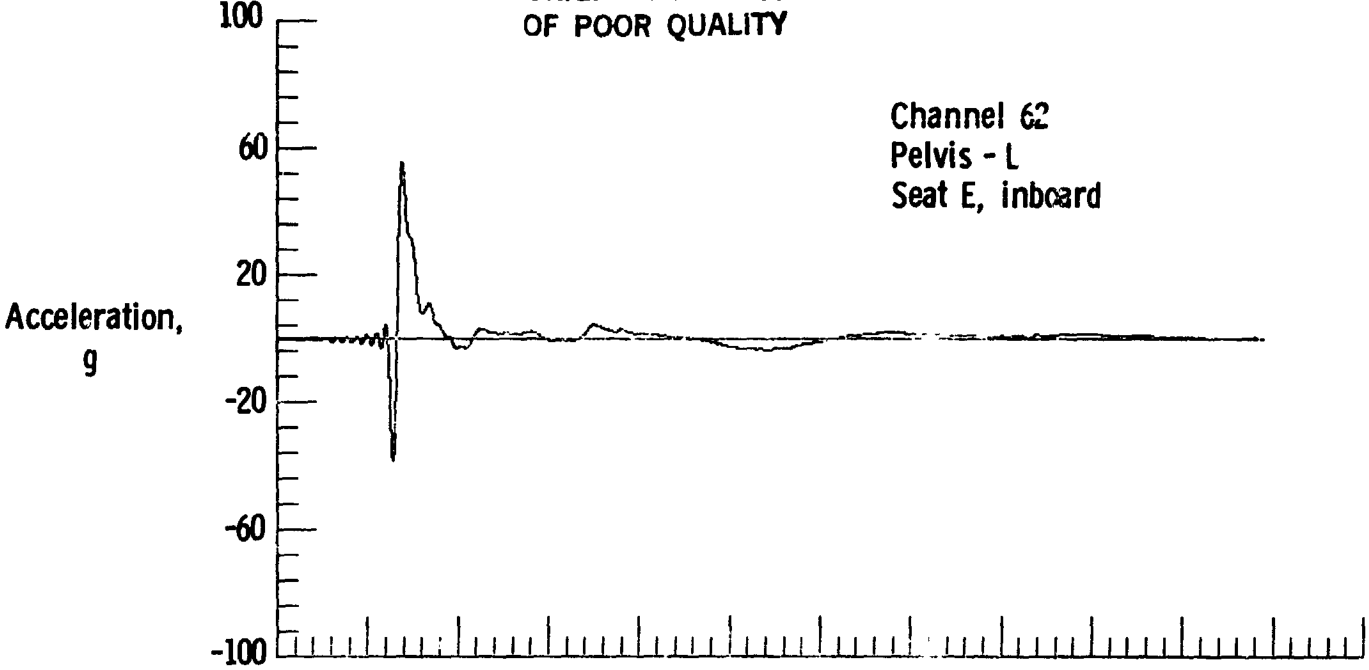

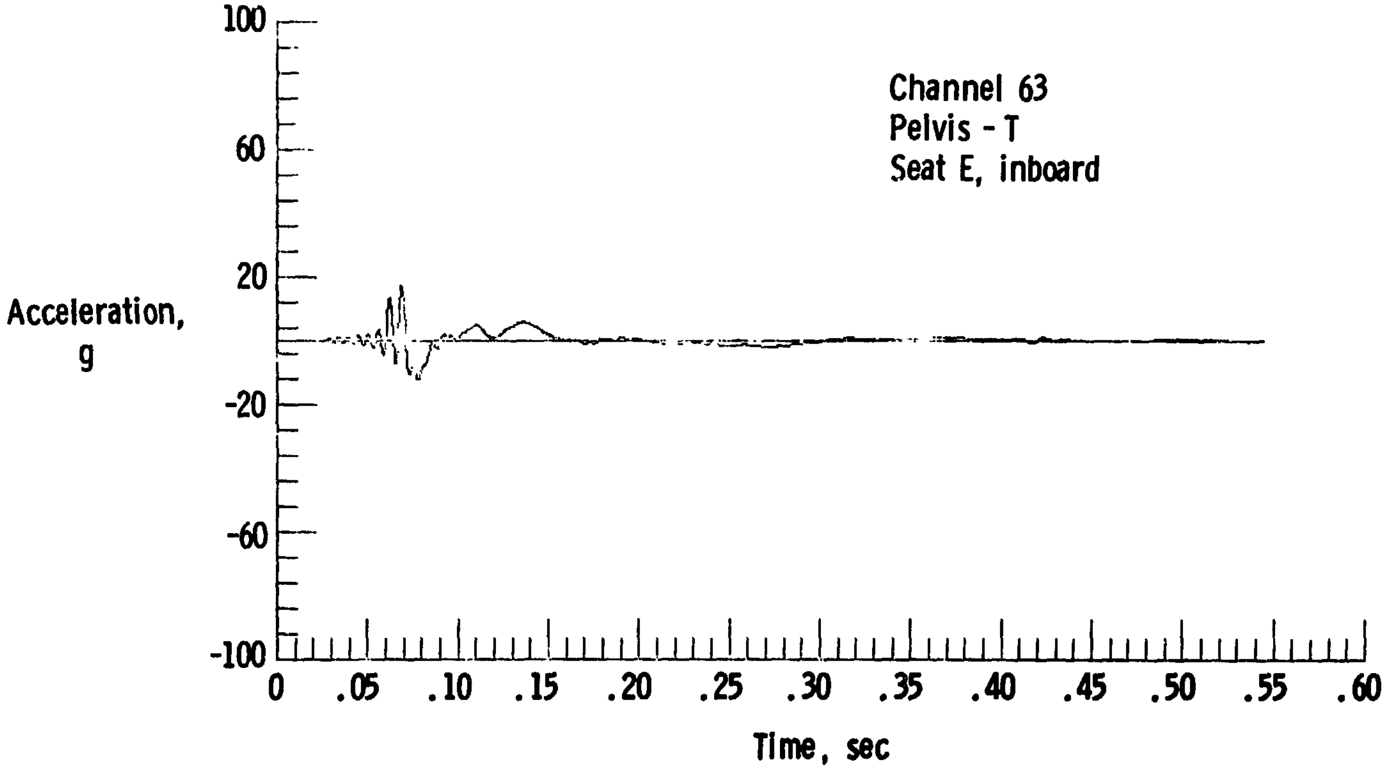

Figure 10.- Continued.

(l) Occupant accelerations.

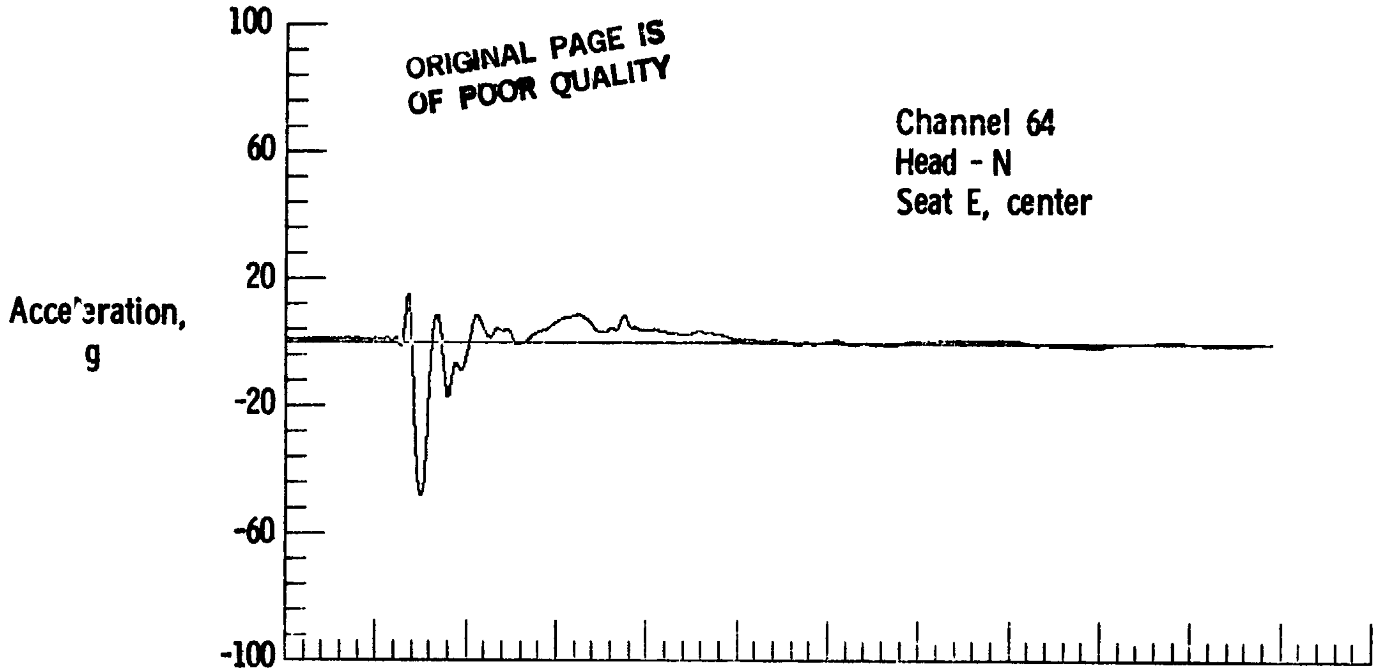

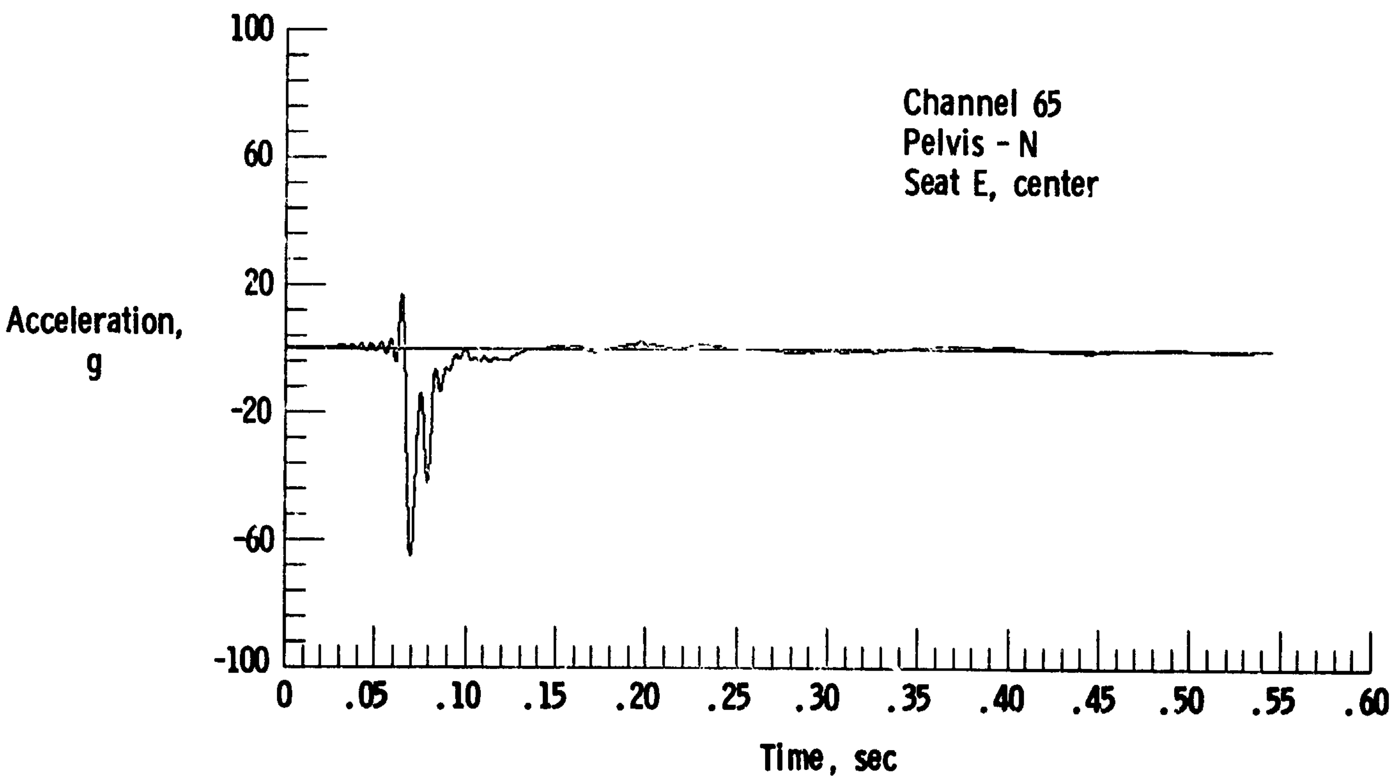

Figure 10.- Continued.

(m) Occupant accelerations.

ORIGINAL PAGE IS
OF POOR QUALITY

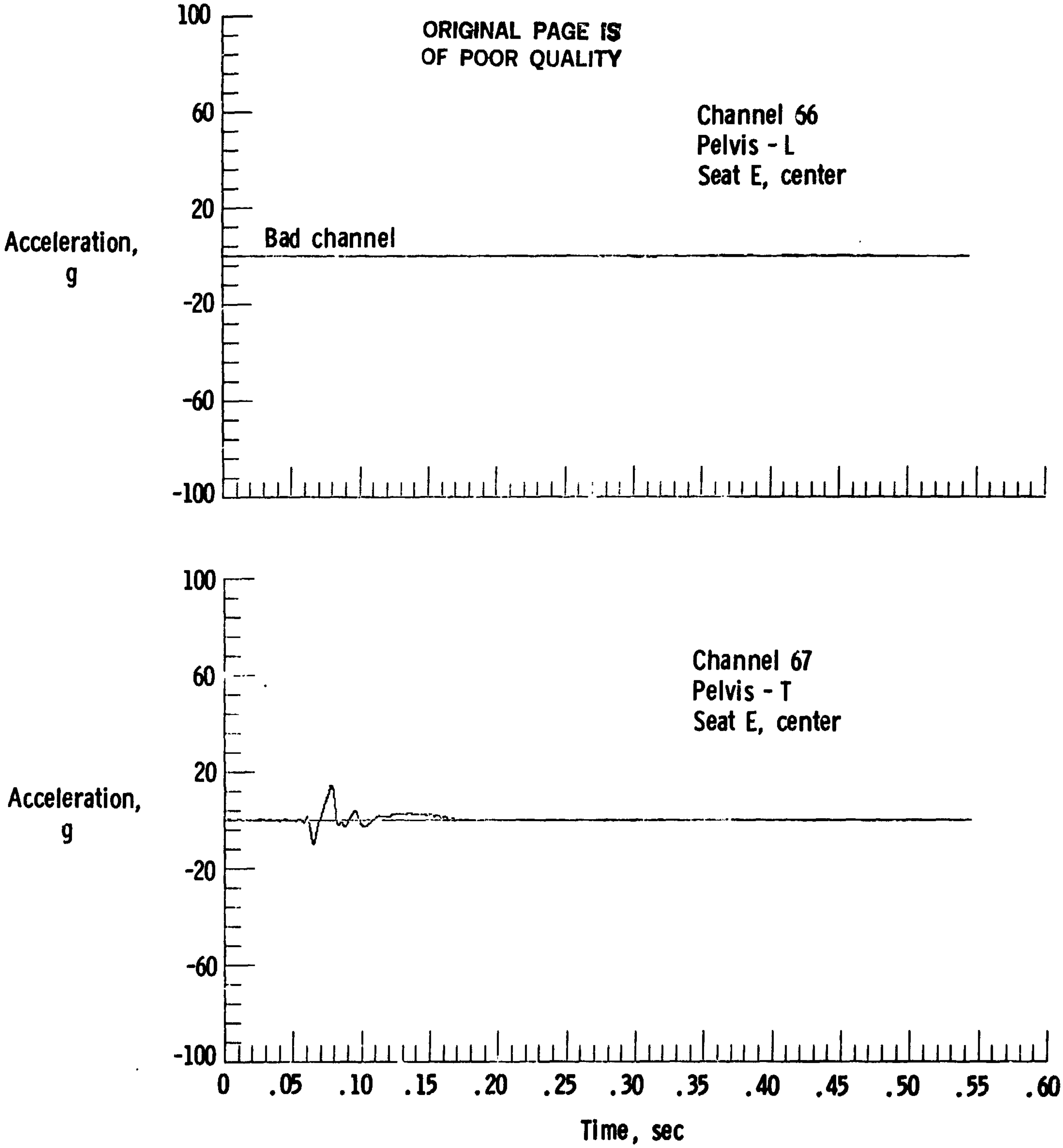

Figure 10.- Continued.

(n) Occupant accelerations.

ORIGINAL PAGE IS
OF POOR QUALITY

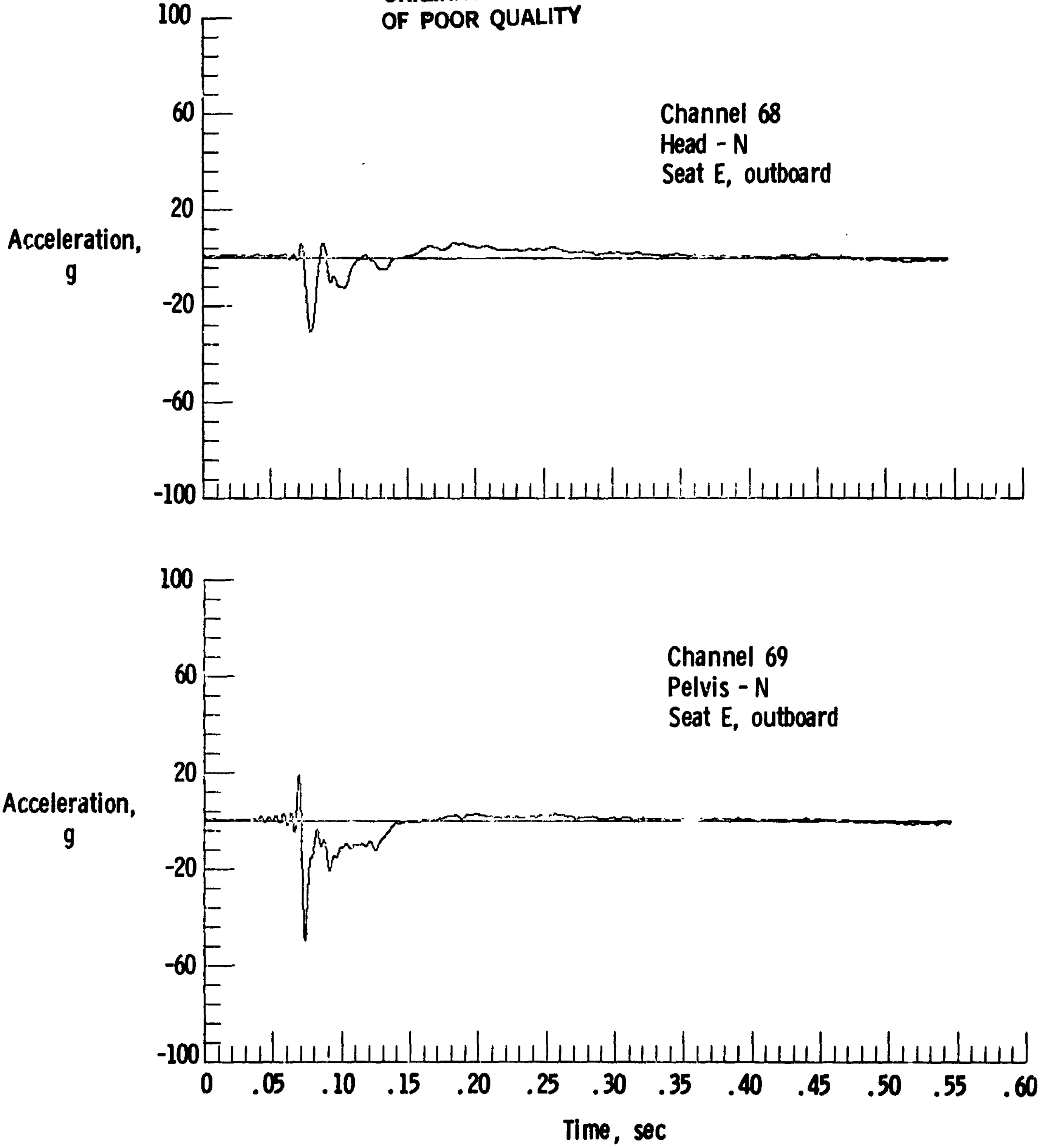

Figure 10.- Continued.

(o) Occupant accelerations.

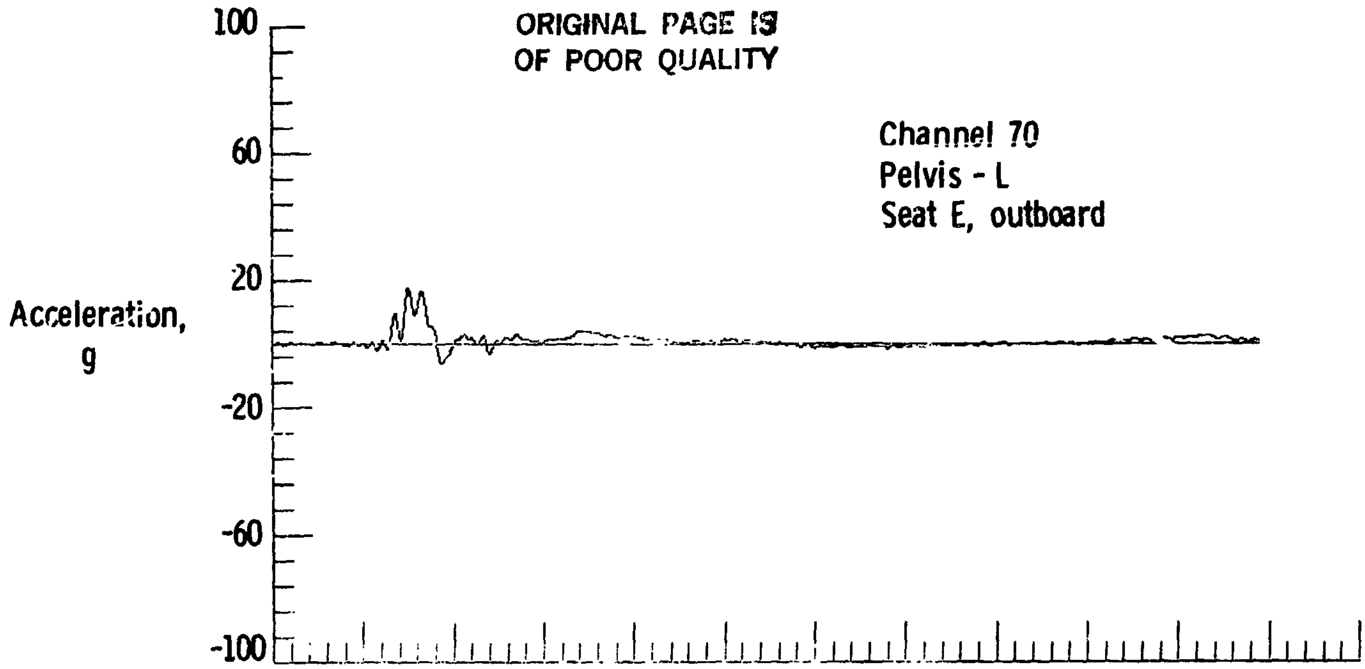

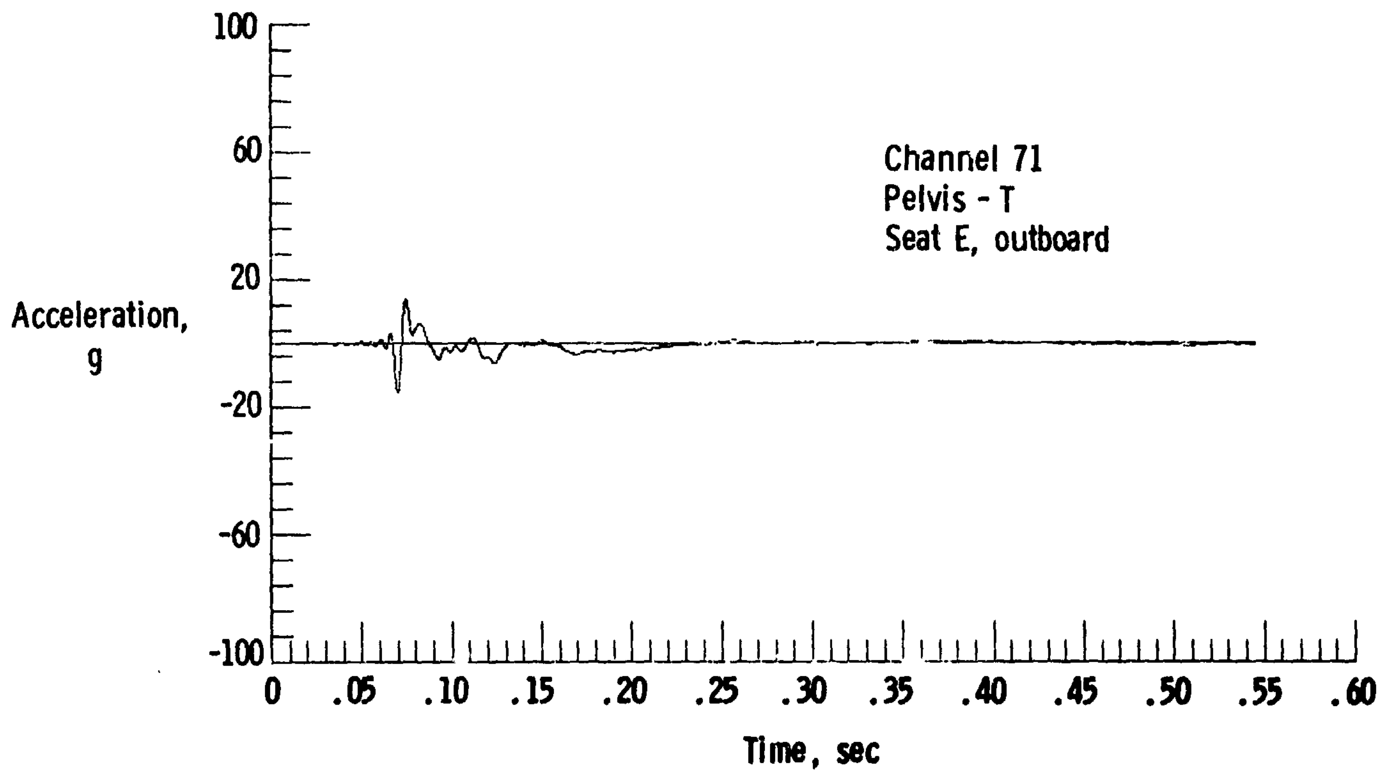

Figure 10.- Concluded.

(p) Occupant accelerations.

ORIGINAL PAGE IS
OF POOR QUALITY

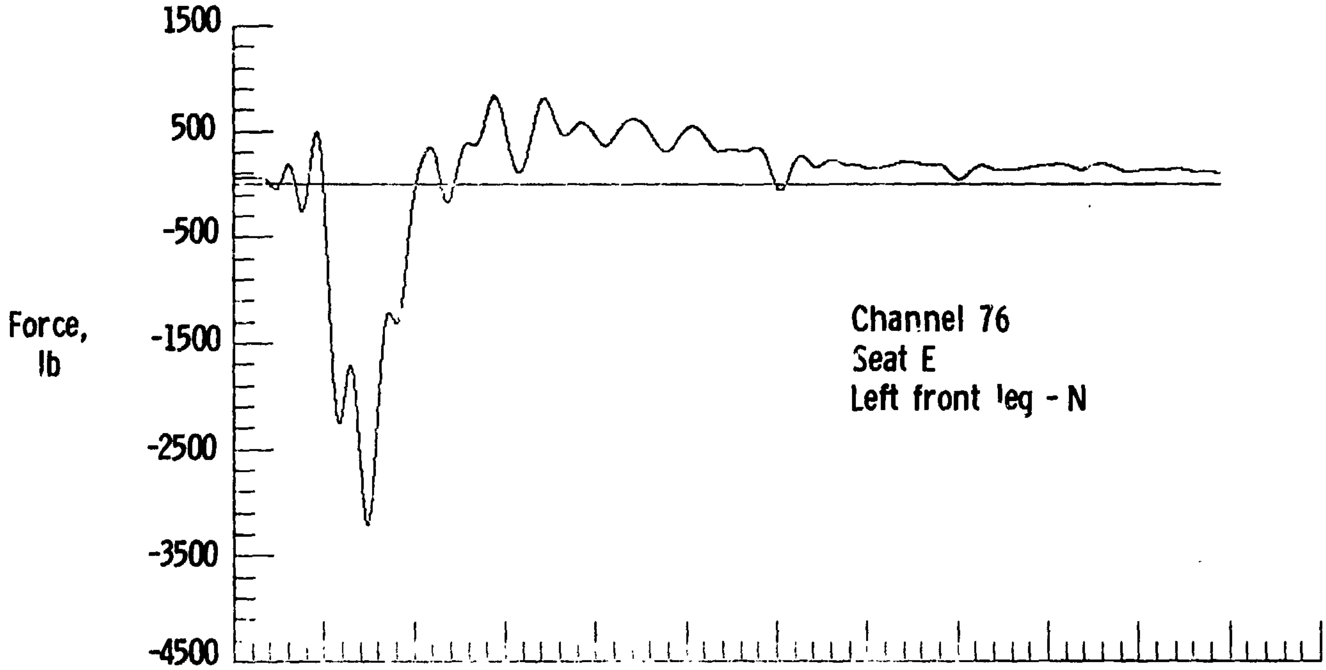

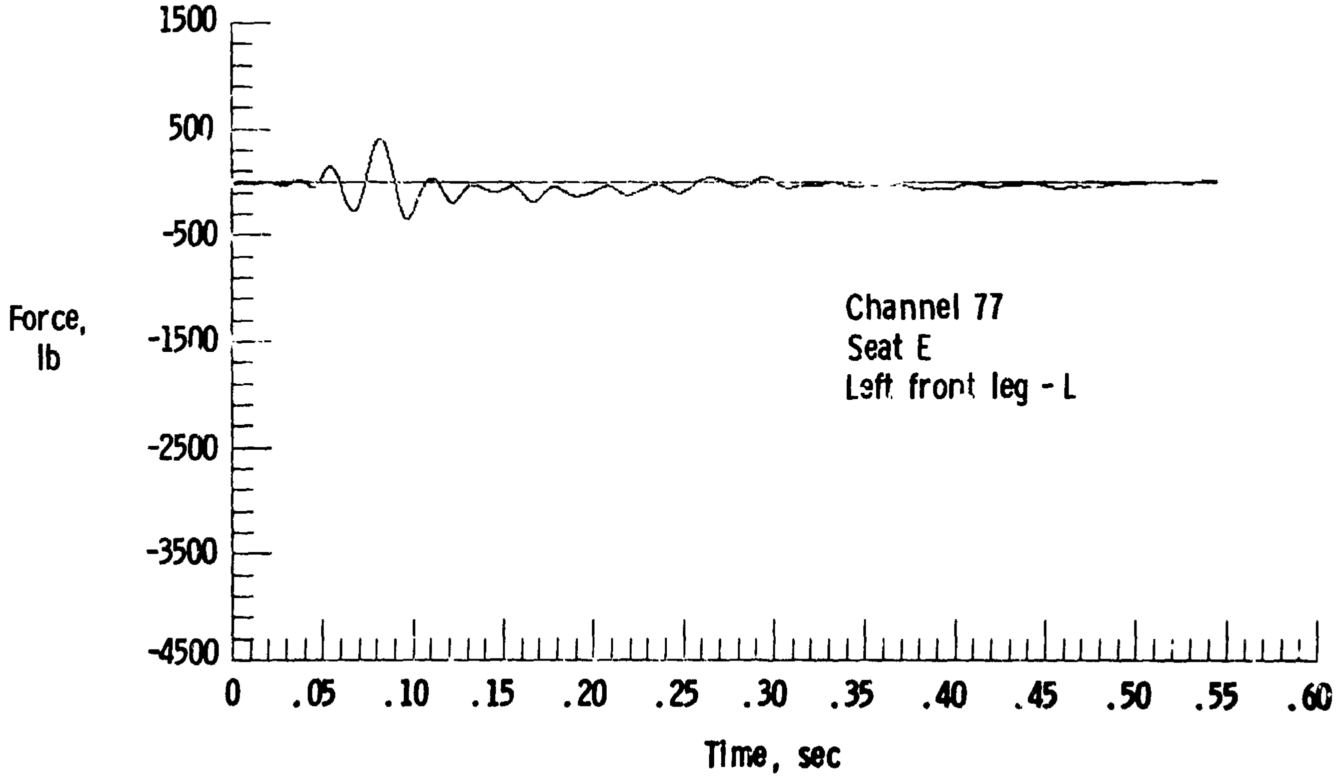

(a) Reaction forces at left front leg.

Figure 11.- Reaction forces measured at seat attachment points.

ORIGINAL PAGE IS
OF POOR QUALITY

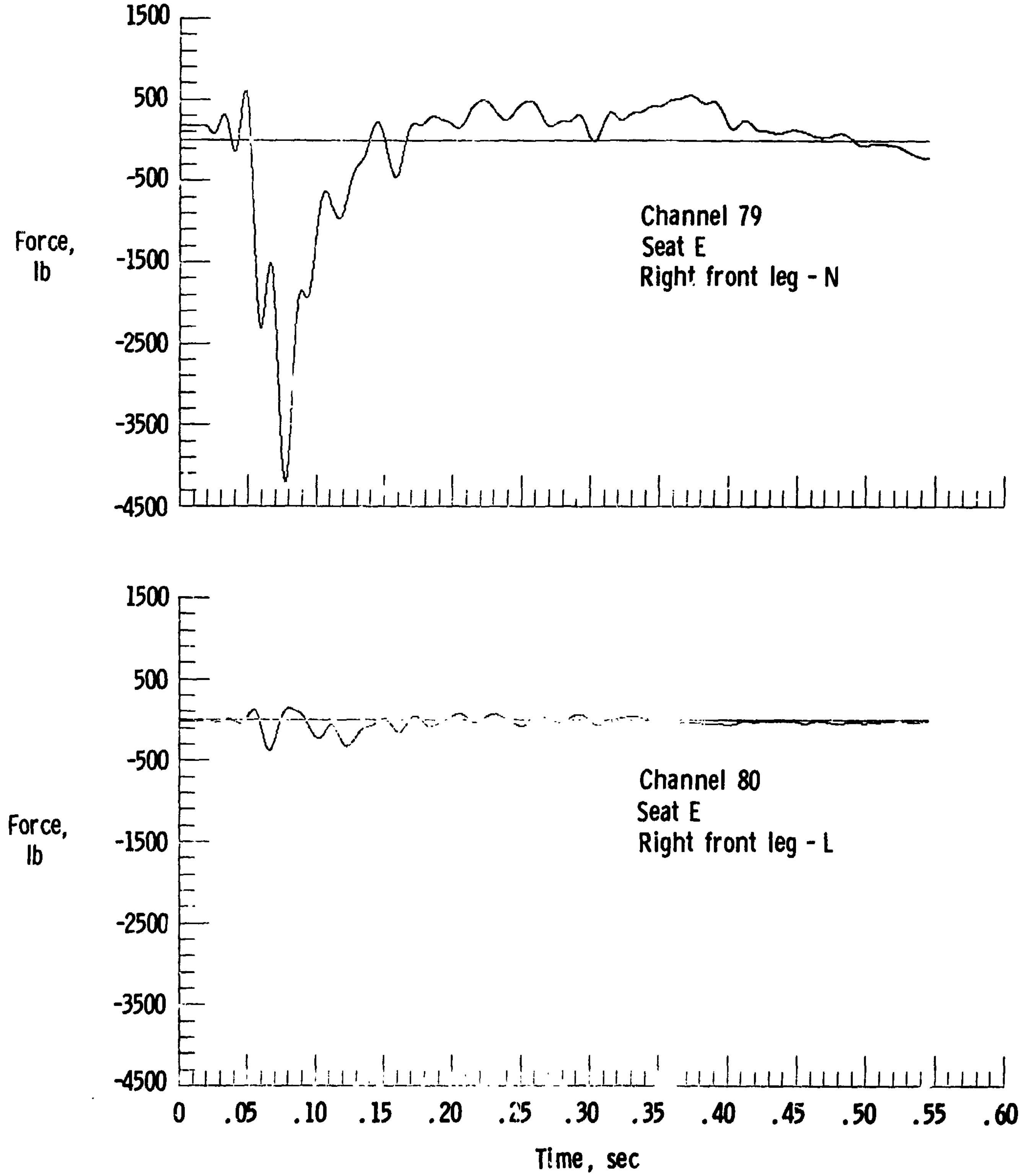

Figure 11.- Continued.

(b) Reaction forces at right front leg.

ORIGINAL PAGE IS
OF POOR QUALITY

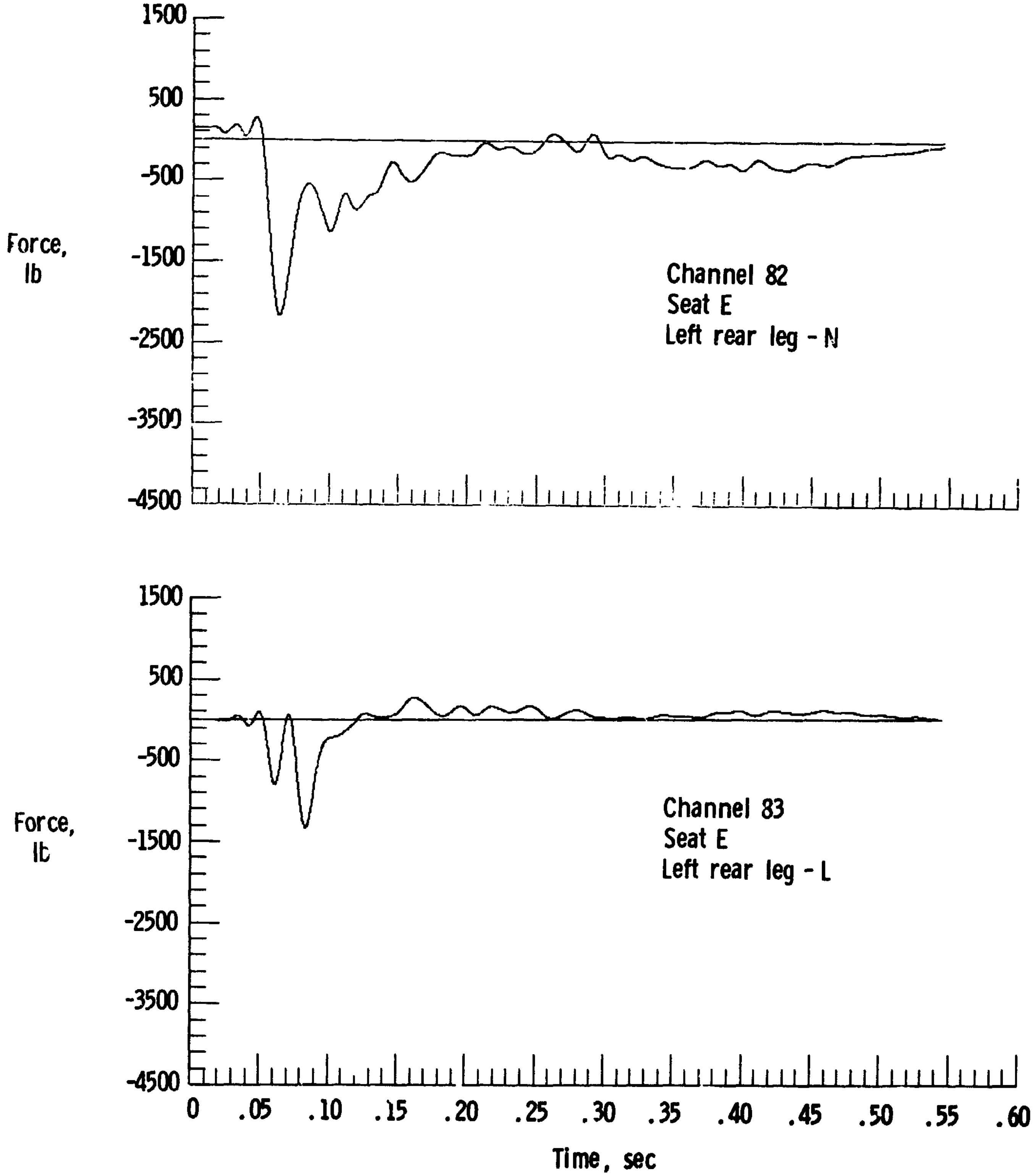

Figure 11.- Continued.

(c) Reaction forces at left rear leg.

ORIGINAL PAGE IS
OF POOR QUALITY

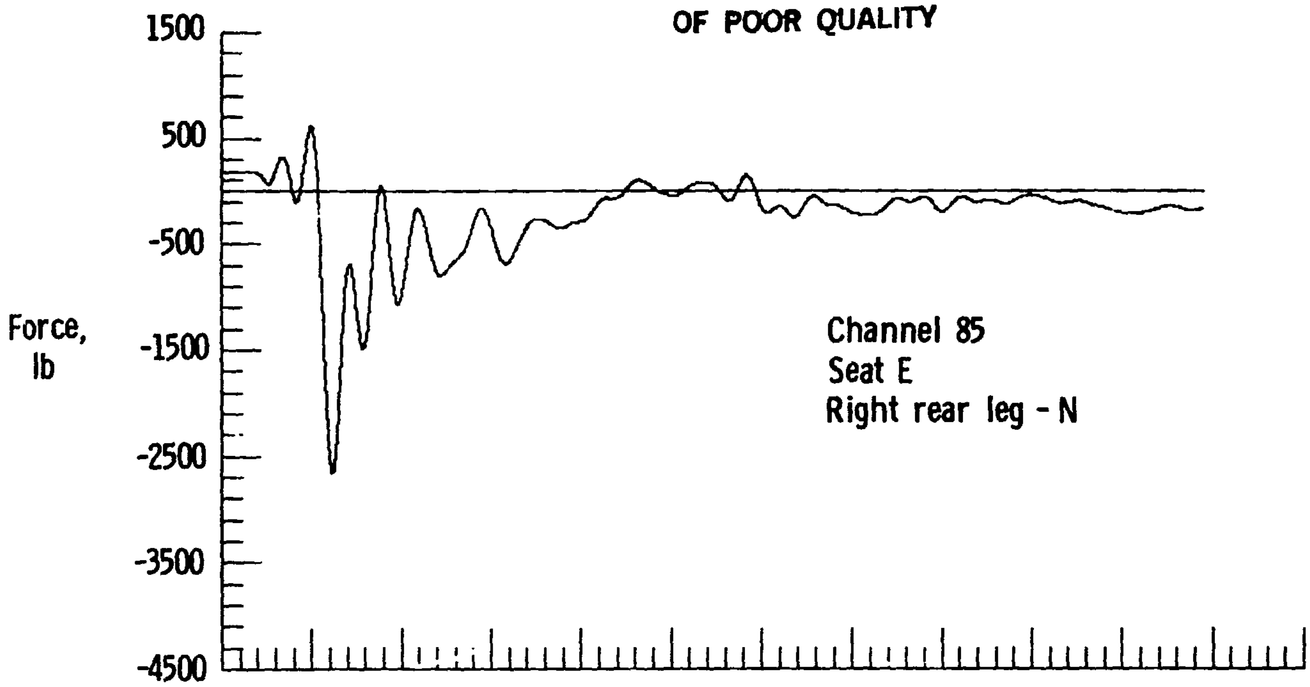

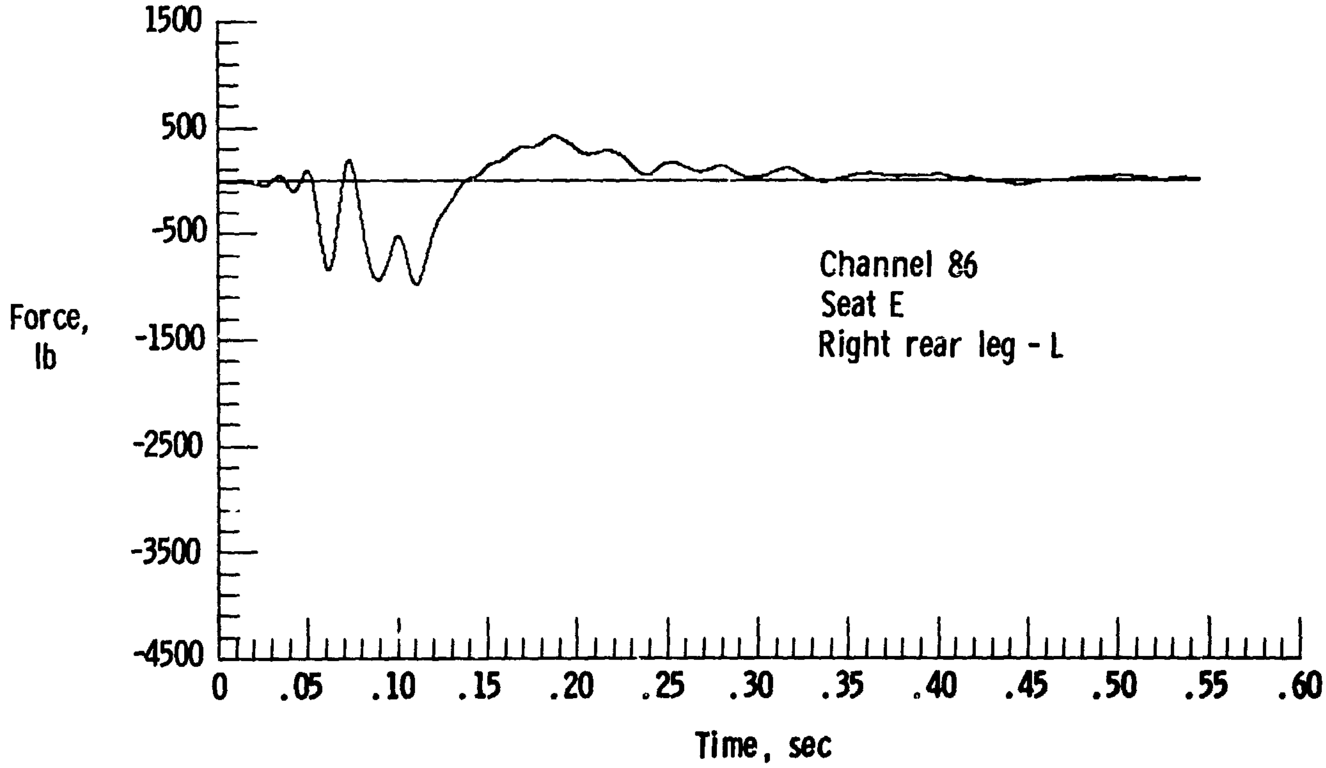

Figure 11.- Concluded.

(d) Reaction forces at right rear leg.